NASA TECHNICAL NOTE

NASA TN D-4929

NASA TN D-4929

THEORY FOR COMPUTING SPAN LOADS AND STABILITY DERIVATIVES DUE TO SIDESLIP, YAWING, AND ROLLING FOR WINGS IN SUBSONIC COMPRESSIBLE FLOW

by M. J. Queijo

Langley Research Center
Langley Station, Hampton, Va.

NATIONAL AERONAUTICS AND SPACE ADMINISTRATION • WASHINGTON, D. C. • DECEMBER 1968

NASA TN D-4929

THEORY FOR COMPUTING SPAN LOADS AND STABILITY DERIVATIVES DUE TO SIDESLIP, YAWING, AND ROLLING FOR WINGS IN SUBSONIC COMPRESSIBLE FLOW

By M. J. Queijo

Langley Research Center
Langley Station, Hampton, Va.

NATIONAL AERONAUTICS AND SPACE ADMINISTRATION

For sale by the Clearinghouse for Federal Scientific and Technical Information
Springfield, Virginia 22151 – CFSTI price $3.00

Page Intentionally Left Blank

THEORY FOR COMPUTING SPAN LOADS AND STABILITY DERIVATIVES DUE TO SIDESLIP, YAWING, AND ROLLING FOR WINGS IN SUBSONIC COMPRESSIBLE FLOW*

By M. J. Queijo
Langley Research Center

SUMMARY

A method of computing span loads and some of the resulting aerodynamic derivatives for wings in sideslip, yawing, and rolling flight is derived. The method is applicable to wings of arbitrary planform, and accounts for compressibility effects. The span-load computations require that angle-of-attack span-load distributions be available for the wing under consideration. The theory developed is a consistent approach, based on the use of a vortex system, for determining the various wing parameters.

INTRODUCTION

The aerodynamic span loads and stability derivatives are important in relation to structural integrity and inherent stability of airplanes. The lifting surfaces (wing and tail surfaces) generally produce the predominant aerodynamic forces; therefore, much effort has been expended in developing methods of predicting the aerodynamics of lifting surfaces. Most of this effort, however, has been directed toward determination of aerodynamic characteristics associated with angle of attack. Aerodynamics associated with other aircraft motions (rolling, yawing, pitching, and sideslipping) have been investigated to a lesser degree, and generally by somewhat cruder methods. This is particularly true for the low-speed regime. For supersonic speeds the nature of the governing equations is such that it has been possible to obtain equations for loads and aerodynamic derivatives for wings performing various modes of motion. (See refs. 1 to 4, for example.) In certain limiting cases it is possible to use supersonic theory to predict subsonic characteristics. (See ref. 4, for example.)

---

*A preliminary version of the material presented herein was included in a dissertation entitled "A Theory and Method of Predicting the Stability Derivatives C_{l_β}, C_{l_r}, C_{n_p}, and C_{Y_p} for Wings of Arbitrary Planform in Subsonic Flow," offered in partial fulfillment of the requirements for the degree of Doctor of Philosophy in Engineering Mechanics, Virginia Polytechnic Institute, Blacksburg, Virginia, June 1963.

There are a number of problems associated with attempting to predict aerodynamic characteristics of wings performing the possible modes of motion. One problem is that of finding an adequate mathematical model for the wing, and the second is that associated with solution of the equations which arise from use of the mathematical models. Various methods for predicting certain aerodynamic characteristics of unswept wings have been developed by a number of investigators, and numerous reports have been published from which certain characteristics can be obtained for specific wings. (See refs. 5 and 6, for example.) Three general approaches have been used in determining the aerodynamics of swept wings. These are:

(a) Computations based on mathematical models associated with the use of vortices, doublets, or other concepts to represent the wing (refs. 7 to 11, for example).

(b) Determination of approximate equations based on treating each wing semispan as one-half of an unswept wing. The fictitious "unswept" panels are skewed to simulate a swept wing (refs. 12 to 15, for example).

(c) Development of design charts based on tests of a great number of wings with various sweep angles, aspect ratios, and taper ratios (ref. 16, for example).

The first of these approaches is generally difficult and in some cases involves the solution of numerous simultaneous equations. For these reasons, only a few aerodynamic parameters $\left(\text{primarily aerodynamic-center position, } C_{L_\alpha}, \text{ and } C_{l_p}\right)$ have been attacked by fairly rigorous methods. The use of high-speed computers to solve many simultaneous equations has permitted the numerical solution of equations better defining the wing boundary, but solutions generally have been obtained for angle-of-attack loading.

The second approach has been quite successful in predicting trends, and with some modifications has been used to obtain good quantitative results for certain aerodynamic characteristics. (See ref. 15, for example.)

The third approach is adequate for engineering data, provided the available data envelop the range of geometric variables of interest. Unfortunately, the amount of data available for some of the wing derivatives is very limited because of the scarcity of experimental facilities for determining such derivatives.

The purpose of the present paper is to examine the problem of wing characteristics in subsonic compressible flow and to develop a consistent method for computing these characteristics.

The method developed herein is a new approach for estimating span loads and the derivatives C_{l_β}, C_{l_r}, C_{l_p}, C_{n_p}, and C_{Y_p} for wings of arbitrary planform in subsonic compressible flow. It is based on a vortex representation of the wing which was first developed by the author for sideslipping wings in incompressible flow (ref. 17).

Results are generally applicable to the low angle-of-attack region, where the various wing characteristics vary linearly with angle of attack or lift coefficient.

SYMBOLS

A aspect ratio, b^2/S

a_o two-dimensional lift-curve slope

b wing span

C_L wing lift coefficient, $\frac{L}{\frac{1}{2}\rho V^2 S}$

C_{L_α} wing lift-curve slope, $\frac{\partial C_L}{\partial \alpha}$, per radian

C_l rolling-moment coefficient, $\frac{M_X}{\frac{1}{2}\rho V^2 Sb}$

$C_{l_p} = \frac{\partial C_l}{\partial \frac{pb}{2V}}$

$C_{l_r} = \frac{\partial C_l}{\partial \frac{rb}{2V}}$

$C_{l_\beta} = \frac{\partial C_l}{\partial \beta}$

C_n yawing-moment coefficient, $\frac{M_Z}{\frac{1}{2}\rho V^2 Sb}$

$C_{n_p} = \frac{\partial C_n}{\partial \frac{pb}{2V}}$

C_Y side-force coefficient, $\frac{F_Y}{\frac{1}{2}\rho V^2 S}$

$C_{Y_p} = \dfrac{\partial C_Y}{\partial \dfrac{pb}{2V}}$

c wing local chord

$\bar{c}$ wing average chord

c_l section lift coefficient, $\dfrac{\text{Section lift}}{\frac{1}{2}\rho V^2 c}$

c_{l_α} section lift-curve slope, $\dfrac{\partial c_l}{\partial \alpha}$

$\left(c_{l_\alpha}\right)_\alpha$ three-dimensional section lift-curve slope for wing at angle of attack

$\left(c_{l_\alpha}\right)_p$ effective three-dimensional section lift-curve slope for rolling wing

$\left(\dfrac{cc_l}{\bar{c}C_L}\right)$ parameter for section lift, per unit lift coefficient

$\left(\dfrac{cc_l}{\bar{c}C_{L_\beta}}\right)$ parameter for incremental section lift due to sideslip, for a wing at angle of attack

$\left(\dfrac{cc_l}{\bar{c}\dfrac{pb}{2V}}\right)$ parameter for incremental section lift due to rolling

$\left(\dfrac{cc_l}{\bar{c}C_L\dfrac{rb}{2V}}\right)$ parameter for incremental section lift due to yawing, for a wing at angle of attack

c_r wing root chord

c_t wing tip chord

D spanwise distance from wing root chord to center of rotation of yawing wing

F_Y side force

$(f_Y)_1$	side force associated with a chordwise-bound vortex
$(f_Y)_2$	side force associated with quarter-chord-line vortex
L	lift
l_2	lift per unit length of chordwise-bound vortex
l_y	lift per unit span of quarter-chord-line vortex
l_ξ	lift per unit length of quarter-chord-line vortex
M	free-stream Mach number
M_N	Mach number of free stream normal to wing quarter-chord line
M_X	rolling moment
M_Z	yawing moment
p	rate of roll, radians per second
r	yawing angular velocity, radians per second
S	wing area
u	wind velocity in x-direction
V	free-stream wind velocity relative to wing center of gravity
V_l	local velocity
V_N	free-stream wind velocity normal to wing quarter-chord line
v	wind velocity in y-direction
X,Y	longitudinal and spanwise reference axes, with origin at center of gravity
x,y	distances along reference axes

x_{ac} chordwise distance between aerodynamic center (a.c.) and moment center (or center of gravity, c.g., in flight), positive when c.g. is upstream of a.c.

x_c x-distance to wing trailing edge

$x_{c/4}$ x-distance to quarter-chord line

$\bar{y}$ spanwise position of centroid of the angle-of-attack span loading

$\tilde{y}$ radius of gyration of angle-of-attack span loading

α angle of attack (or incidence), radians

β sideslip angle, radians

Γ_y circulation strength related to spanwise position

Γ_ξ circulation strength related to displacement along quarter-chord line

δ local effective sideslip angle due to yawing, radians

ϵ infinitesimal displacement in spanwise direction

Λ sweep angle of quarter-chord line, radians

λ wing taper ratio, c_t/c_r

ξ distance along the quarter-chord line, measured from wing root chord

ρ mass density of air

Subscripts:

M compressible flow

M=0 incompressible flow

p part due to rolling

r part due to yawing

α part due to angle of attack

β part due to sideslip

A star (*) indicates that the quantity has been nondimensionalized by division by $b/2$; for example, $y^* = \frac{y}{b/2}$.

VORTEX SYSTEM

The vortex system used in this analysis is for essentially a modified lifting-line-theory approach, and is illustrated in figure 1. The system consists of a bound vortex along the wing quarter-chord line and a bound-vortex sheet from the quarter-chord line to the wing trailing edge. Behind the wing trailing edge, the vortex sheet is in the direction of the airstream. This system was applied to sideslipping wings in reference 17, and proved to be quite accurate in predicting the parameter C_{l_β} for a wide range of wings in subsonic, incompressible flow. An appraisal of this vortex system indicated that it would be applicable to the estimation of other wing derivatives.

The vortex system adopted for this study allows the possibility of lift generation by the bound vortices, which are:

(a) The quarter-chord-line vortex, which extends across the entire wing span

(b) The chordwise-bound vortices, which are parallel to the wing plane of symmetry and extend from the wing quarter-chord line to the wing trailing edge.

The trailing vortex sheet behind the wing is made up of "free" vortices which are in the direction of the airstream and hence develop no lift.

CIRCULATION DISTRIBUTION

The strength of the chordwise-bound vortices is determined by the gradient of the strength distribution of the quarter-chord-line vortex; therefore, the lift distribution of the wing can be determined if the vortex strength distribution of the quarter-chord line is known and if the wind velocity components are known. The distribution of the wind velocity components relative to the wing can be determined easily for each possible motion of the wing. The basic problem in determining wing load distribution, therefore, is that of determining the vortex (or circulation) distribution for all wing motions. The three types of motion considered in this paper are sideslip, yawing, and rolling.

Sideslipping Wing

The sideslipping wing was studied in reference 17. It was argued therein that the circulation distribution in sideslip was essentially the same as that for a wing in zero sideslip. Thus zero-sideslip circulation distributions could be used for estimating aerodynamic loads and the parameter C_{l_β} for wings in sideslip. The vortex system for the wing in sideslip and the direction of the airflow are shown in figure 2.

Yawing Wing

The bound-vortex pattern of the yawing wing is the basic pattern shown in figure 1. The trailing-free vortex sheet, however, is curved to match the airflow streamlines (fig. 3). An examination of the flow pattern over the wing (fig. 4) shows that there is a lateral velocity component resulting from the flow curvature, and that the magnitude of the component is a function of position on the wing. The wing therefore can be considered to be in sideslip, with the effective sideslip angle varying over the wing. The arguments presented with regard to circulation distribution of the wing in sideslip can be carried over to the yawing wing. An assumption of the present theory is that the circulation distribution for a yawing wing is essentially the same as that for a nonyawing wing.

Rolling Wing

The problem of circulation distribution for the rolling wing is somewhat different from that for the sideslipping and yawing wing. In the case of the rolling wing, the local geometric angle of attack is increased by

$$\Delta\alpha = \frac{py}{V}$$

The primary cause of circulation, and hence the circulation itself, is altered by rolling. The net circulation of a rolling wing, therefore, is made up of:

(a) Circulation due to the symmetric angle of attack

(b) Circulation due to the antisymmetric angle-of-attack distribution associated with rolling velocity

The assumed wing vortex system and the circulation distributions that have been discussed form the basis for the present theory for the computation of wing aerodynamic characteristics.

PRESENTATION OF RESULTS

General Remarks

General equations are derived in appendix A for the span loads and certain aerodynamic characteristics associated with sideslipping, yawing, and rolling for wings of arbitrary planform. These equations are applicable in the low angle-of-attack region, where the characteristics vary linearly with angle of attack and lift coefficient. Span loads associated with sideslip, yawing, and rolling can be obtained by the methods presented herein only if the angle-of-attack span load is known. Such information is available for a wide range of wing geometry (ref. 18, for example). The angle-of-attack loading for odd-shaped wings can be obtained by application of the horseshoe-vortex method of references 19 to 22.

The equations of this paper, for incompressible flow, are derived in appendix A. Compressibility effects are derived in appendix B. Some of the pertinent equations are summarized in appendix C.

Many of the equations derived herein involve the spanwise position of the centroid and radius of gyration of the angle-of-attack loading of the wing semispan. The centroid position for angle-of-attack loadings has been determined for a wide range of wing planforms and is readily available in the literature. (See refs. 8, 18, and 21, for example.) The present theory appears to be the only one in the literature in which the radius of gyration occurs as a factor in determining aerodynamic characteristics. It was necessary, therefore, to compute the radius of gyration $\tilde{y}^*$ for use in this paper. The values were determined by plotting the product $\left(\frac{cc_l}{\bar{c}C_L}\right)(y^*)^2$ against y^* for a large number of wings and performing a mechanical integration to obtain $\tilde{y}^*$ by use of the following equation:

$$(\tilde{y}^*)^2 = \int_0^1 \left(\frac{cc_l}{\bar{c}C_L}\right)(y^*)^2 dy^* \tag{1}$$

A total of 160 such integrations were performed to obtain the desired coverage of wing planforms. Values of $\bar{y}^*$ and of $\tilde{y}^*$ are plotted in figures 5 and 6 as functions of sweep, aspect ratio, and taper ratio for use in this paper and for general information. Data for the span loads were obtained from reference 18.

Span-Load Distributions

The span-load equations derived in this paper are applicable for the determination of the incremental load due to sideslip, yawing, or rolling velocity of a wing for which the

span load in symmetric flight is known. The span-load equations are summarized in appendix C. Equations (C1) to (C3) are very general and should be used if the sweep angle varies across the wing span. In such instances it may not be possible to find in the literature the corresponding angle-of-attack loading of the wing. In these instances, as noted previously, the angle-of-attack loading can be determined in a straightforward manner (solution of simultaneous algebraic equations) by the method of reference 19, 20, or 21.

If sweep is constant across the span, equations (C4) to (C6) are applicable and more convenient. In these cases the angle-of-attack span-load distribution can be obtained from a number of sources, such as reference 18.

Most of the theoretical angle-of-attack span-load distributions available in the literature have been determined by use of the Weissinger method. It is of interest and significance that angle-of-attack span loadings determined by the use of horseshoe vortices (as in ref. 19 or 20) will closely approximate loadings from the Weissinger method if a minimum of about 20 horseshoe vortices are used to represent the wing. (See ref. 19.) The horseshoe-vortex method is applicable for representing wings having discontinuities in sweep distribution (for example, M- or W-wings), where the applicability of the Weissinger method is doubtful. This horseshoe-vortex method was used in reference 22 to determine the span loads of some M- and W-wings, and can be used for wings of arbitrary planform. The system of horseshoe vortices was also used in reference 17 to obtain the loads on sideslipping wings. In such a case, the loads are obtained from either a mechanical integration or from summing terms of a series expansion (ref. 17).

Aerodynamic Coefficients

The equations derived for the various aerodynamic coefficients are presented in appendix C. Equations (C7) to (C11) are very general and are applicable to wings of arbitrary planform. If sweep is constant across the semispan, and if the chord is a linear function of spanwise position, equations (C12) to (C16) are applicable and convenient.

Equations (C12) to (C16) have been used to construct a series of figures from which numerical values of the various coefficients for a Mach number of zero can be obtained as a function of wing geometry. The effect of Mach number can be obtained through use of equations (C12) to (C16). The parameters for a Mach number of zero are presented in the following figures: C_{l_β}/C_L in figure 7; C_{l_r}/C_L in figure 8; C_{l_p} in figure 9; C_{Y_p}/C_L in figure 10; and C_{n_p}/C_L in figure 11.

DISCUSSION OF RESULTS

Sideslipping Wing

The span load due to sideslip can be computed by equation (C1) or (C4). No other method appears to be available for estimating these loads. Experimental data are also almost nonexistent, except for the sideslip data given in reference 23 for a wing in incompressible flow. As shown in reference 17, these data compared well with the incompressible-flow equation of the present theory.

The rolling-moment parameter associated with sideslip for a trapezoidal wing in compressible flow is given by equation (C12), repeated here for convenience:

$$\frac{C_{l_\beta}}{C_L} = -\frac{1}{2}\left[\frac{3}{A(1+\lambda)} + \bar{y}^*\left(\tan\Lambda - \frac{6}{A}\frac{1-\lambda}{1+\lambda}\right)\right] + 0.05$$

$$-\frac{1}{2}\bar{y}^* \frac{A^2M^2\tan\Lambda}{\left[\left(\frac{A}{\cos\Lambda}\right)^2 - A^2M^2 + 4\right]^{1/2}\left\{2 + \left[\left(\frac{A}{\cos\Lambda}\right)^2 - A^2M^2 + 4\right]^{1/2}\right\}} \qquad (2)$$

The analysis of reference 17 shows that this equation is quite accurate for wings in incompressible flow.

Very little theoretical work has been done to determine compressibility effects on the derivatives investigated in this paper. The Prandtl-Glauert transformation is applicable for symmetric flow, but there are a number of fundamental questions regarding its application if the flow about the wing is not symmetric. The Prandtl-Glauert transformation can be applied either as a change in section lift-curve slope or as a change in wing geometry in symmetric flow. In unsymmetric flow, a geometric change in accordance with the Prandtl-Glauert transformation results in a distorted wing shape – that is, the transformed wing semispans are different from each other. This basic problem of application can be avoided, as was done in reference 14, by assuming that each wing semispan is one-half of a wing in symmetric flow. The compressibility corrections are then applied to each wing semispan and the loads of each semispan are used to obtain the wing characteristics.

A somewhat simpler approach was used in reference 24, where the author simply chose to modify the section lift-curve slope as if the actual wing were in symmetric flow.

It does not appear possible to obtain a direct evaluation of the estimated compressibility effects on the values of C_{l_β}/C_L for an isolated wing, since high-speed data are

generally obtained for wing-fuselage combinations. However, wing-fuselage data would be expected to have about the same trends as wing-alone data. Figure 12 shows experimental compressibility effects for several wing-body combinations and compares the results with those predicted by the wing-alone theory of reference 14 and by equation (2) of the present paper. The data and theories all show an increase in the magnitude of C_{l_β}/C_L with increase in Mach number. The effect on wing-fuselage data is somewhat smaller than that predicted by the wing-alone theories. Reference 14 suggests an empirical method for accounting for the fuselage. However, as pointed out in that reference, additional effort is required to define more precisely the effects of the fuselage on C_{l_β}/C_L.

Yawing Wing

The span loads due to yawing can be determined from equations (C2) and (C5). The author could find no other theory or experimental results to compare with these equations.

The derivative obtained for the yawing wing is C_{l_r}. For a trapezoidal wing in compressible flow it is given by

$$\frac{C_{l_r}}{C_L} = \left[\frac{1}{2}\left(1 + \tan^2\Lambda\right) - \frac{9}{2A}\frac{1-\lambda}{1+\lambda}\tan\Lambda + \frac{27}{4A^2}\left(\frac{1-\lambda}{1+\lambda}\right)^2\right]\left(\bar{y}^*\right)^2 + \left(\frac{3}{A}\frac{1-\lambda}{1+\lambda}\tan\Lambda - \frac{\tan^2\Lambda}{2}\right)\left(\bar{y}^*\right)^2$$

$$+ \left[\frac{3\tan\Lambda}{2A(1+\lambda)} - \frac{9(1-\lambda)}{A^2(1+\lambda)^2}\right]\bar{y}^* + \left(\frac{\tan\Lambda}{2} - \frac{3}{A}\frac{1-\lambda}{1+\lambda}\right)x_{ac}^*\bar{y}^* + \frac{3x_{ac}^*}{2A(1+\lambda)} + \frac{9}{4A^2(1+\lambda)^2}$$

$$+ \frac{A^2M^2}{2}\frac{-\left(\bar{y}^*\right)^2\tan^2\Lambda + \left(\bar{y}^*\right)^2\left(1+\tan^2\Lambda\right) + x_{ac}^*\bar{y}^*\tan\Lambda}{\left[\left(\frac{A}{\cos\Lambda}\right)^2 - A^2M^2 + 4\right]^{1/2}\left\{2 + \left[\left(\frac{A}{\cos\Lambda}\right)^2 - A^2M^2 + 4\right]^{1/2}\right\}} \qquad (3)$$

Although this derivative is important in determining the dynamic lateral stability of aircraft, there is little published information on theoretical or experimental values of C_{l_r}. Some incompressible-flow information is available from references 5 and 12. However, reference 5 is applicable only to unswept wings. Figure 13 shows comparisons of experimental data (incompressible flow) with the theory of reference 12 and with equation (3) of the present paper. Both theories fit the data equally well.

Reference 24 and equation (3) both predict an increase in C_{l_r}/C_L with increase in Mach number, as shown in figure 14, but no experimental data are available for comparison.

Rolling Wing

The equation for additional load due to rolling velocity is, for a trapezoidal wing in compressible flow,

$$\left(\frac{cc_l}{\bar{c}\,\frac{pb}{2V}}\right)_{M,\alpha} = \left(\frac{cc_l}{\bar{c}C_L}\right)_{M,\alpha} y^* \frac{\pi A}{2 + \left[\left(\frac{A}{2\cos\Lambda}\right)^2 - \frac{A^2M^2}{4} + 4\right]^{1/2}} \tag{4}$$

This type of loading is amenable to solution by the Weissinger method (ref. 25). Comparisons of span load due to rolling as obtained by equation (4) and from reference 25 are shown in figure 15. The agreement between the two theories is quite good for incompressible flow.

The span load distribution can be used to obtain the parameters C_{l_p}, C_{Y_p}, and C_{n_p}, and these are given by the equations

$$C_{l_p} = -\frac{1}{2}\left(\tilde{y}^*\right)^2 \frac{\pi A}{2 + \left[\left(\frac{A}{2\cos\Lambda}\right)^2 - \left(\frac{AM}{2}\right)^2 + 4\right]^{1/2}} \tag{5}$$

$$\frac{C_{Y_p}}{C_L} = \bar{y}^* \tan\Lambda \tag{6}$$

$$\frac{C_{n_p}}{C_L} = -\frac{1}{2}\left\{\left(\tilde{y}^*\right)^2 + \left[\left(\tilde{y}^*\right)^2 - \left(\bar{y}^*\right)^2\right]\tan^2\Lambda + x^*_{ac}\bar{y}^*\tan\Lambda\right\} \tag{7}$$

Comparisons between equation (5) and experimental results for C_{l_p} are shown in figure 16. Generally there is good agreement between experiment and equation (5), particularly at low aspect ratios.

The derivative C_{Y_p} generally has no effect on the dynamic lateral stability of an airplane and therefore is not important in itself. However, its value is of importance in transforming certain of the other derivatives to various systems of axes. The basic reference for theoretical values of this parameter in incompressible flow is reference 12. Theoretical and experimental results from reference 12 and values from equation (6) are shown in figure 17. Both theories generally underestimate this parameter. The present theory indicates no effect of compressibility on C_{Y_p}/C_L, whereas reference 24 indicates that C_{Y_p}/C_L decreases with Mach number. There appear to be no available data to substantiate either theory.

The wing contribution to C_{n_p} is important with regard to dynamic stability of airplanes. Several methods have been developed for predicting this derivative in incompressible flow. These methods are compared with each other and with experimental data in figure 18. Equation (7) indicates no compressibility effects on C_{n_p}/C_L, whereas the theory of reference 24 indicates a decrease with increasing Mach number. However, there appear to be no experimental data available for determining compressibility effects on C_{n_p}/C_L.

CONCLUDING REMARKS

A theory and method are developed for computing span loads due to sideslip, yawing, and rolling for wings in subsonic compressible flow. The method is applicable to wings of any planform, provided the angle-of-attack load distribution is known. Such information is available in the literature for a wide variety of wing planforms, or can be obtained by straightforward methods. The span load (or circulation) distribution is used to determine the stability derivatives due to sideslip, yawing, and rolling. Derivatives estimated by the method are compared with other theories and experimental results where available and applicable. It is not possible at this time to evaluate the present theory relative to others because of the limited amount of data available – particularly with respect to the derivatives associated with yawing and rolling.

Langley Research Center,
National Aeronautics and Space Administration,
Langley Station, Hampton, Va., July 8, 1968,
126-13-01-50-23.

APPENDIX A

DERIVATION OF EQUATIONS FOR INCOMPRESSIBLE FLOW

The vortex system used in this analysis includes a bound vortex along the quarter-chord line, a bound vortex sheet from the wing quarter-chord line to the wing trailing edge, and free vortices (along streamlines) behind the wing. Interaction of the relative wind with the bound vortices produces forces and moments. Equations for these forces and moments are derived in the following sections. In the derivations, reference is made to the right wing semispan unless otherwise noted.

Sideslipping Wing

The equations for span load and rolling moment for wings in sideslip were derived in reference 17. A few of the equations are included here for completeness and because they are required for the compressible-flow development.

The incremental loading due to sideslip is given by

$$\left(\frac{cc_l}{\bar{c}C_{L_\beta}}\right) = \left(\frac{cc_l}{\bar{c}C_L}\right)_\alpha \tan\Lambda - \frac{3}{4}c^* \frac{d\left(\frac{cc_l}{\bar{c}C_L}\right)_\alpha}{dy^*} \tag{A1}$$

and is antisymmetric over the wing. The resulting rolling-moment parameter is

$$\frac{C_{l_\beta}}{C_L} = -\frac{1}{2}\int_0^1 \left[\left(\frac{cc_l}{\bar{c}C_L}\right)_\alpha \tan\Lambda - \frac{3}{4}c^* \frac{d\left(\frac{cc_l}{\bar{c}C_L}\right)_\alpha}{dy^*}\right] y^* dy^* + 0.05 \tag{A2}$$

where the term 0.05 is a correction obtained in reference 17.

For wings with straight leading and trailing edges the sweep angle is constant and c^* can be expressed as a function of wing span:

$$c^* = \frac{4}{A(1+\lambda)}\left[1 - (1-\lambda)y^*\right] \tag{A3}$$

Equation (A1) therefore can be written as

$$\left(\frac{cc_l}{\bar{c}C_{L_\beta}}\right) = \left(\frac{cc_l}{\bar{c}C_L}\right)_\alpha \tan\Lambda - \frac{3}{A(1+\lambda)}\left[1 - (1-\lambda)y^*\right] \frac{d\left(\frac{cc_l}{\bar{c}C_L}\right)_\alpha}{dy^*} \tag{A4}$$

and equation (A2) can be written as

$$\frac{C_{l_\beta}}{C_L} = -\frac{\tan \Lambda}{2} \int_0^1 \left(\frac{cc_l}{\bar{c}C_L}\right)_\alpha y^* dy^* + \frac{3}{2A(1+\lambda)} \int_0^1 \left[1 - (1-\lambda)y^*\right] \frac{d\left(\frac{cc_l}{\bar{c}C_L}\right)_\alpha}{dy^*} y^* dy^* + 0.05 \quad \text{(A5)}$$

Equation (A5) can be integrated, with the result

$$\frac{C_{l_\beta}}{C_L} = -\frac{1}{2}\left[\frac{3}{A(1+\lambda)} + \bar{y}^*\left(\tan \Lambda - \frac{6}{A}\frac{1-\lambda}{1+\lambda}\right)\right] + 0.05 \quad \text{(A6)}$$

Yawing Wing

The analysis of the yawing wing follows closely that of the wing in sideslip (given in ref. 17) but is more complex because the airflow velocity and direction relative to the vortices are functions of both the spanwise and the chordwise position on the wing.

The total wind velocity at any point on the wing (see fig. 4) is given by

$$V_l = r(D - y)\frac{1}{\cos \delta} \quad \text{(A7)}$$

The components parallel and normal to the wing plane of symmetry are

$$u = -V_l \cos \delta = -r(D - y) \quad \text{(A8)}$$

and

$$v = -V_l \sin \delta = -r(D - y)\tan \delta = -rx \quad \text{(A9)}$$

For the right span of the wing, the component of velocity normal to the wing quarter-chord line is given by

$$V_N = -u \cos \Lambda - v \sin \Lambda$$

or, with substitution of equations (A8) and (A9),

$$V_N = r(D - y)\cos \Lambda + rx_{c/4} \sin \Lambda \quad \text{(A10)}$$

APPENDIX A

If the velocity at the wing center of gravity is denoted by V, then

$$V = rD$$

and equation (A10) can be expressed as

$$V_N = (V - ry)\cos \Lambda + rx_{c/4} \sin \Lambda \tag{A11}$$

The lift per unit length of the quarter-chord-line vortex is given by

$$l_\xi = \rho V_N \Gamma_\xi \tag{A12}$$

As discussed previously, a basic assumption of this analysis is that the circulation distribution is that due to angle-of-attack loading, and is not altered by yawing. The lift per unit length of the quarter-chord-line vortex therefore is given by

$$l_\xi = \rho V_N \left(\Gamma_\xi\right)_\alpha \tag{A13}$$

Similarly, the lift per unit span is given by

$$l_y = \rho V \left(\Gamma_y\right)_\alpha \tag{A14}$$

A unit length of quarter-chord-line vortex covers a span equal to $\cos \Lambda$, so that $l_\xi = l_y \cos \Lambda$. Using this equality, and noting that $V_N = V \cos \Lambda$ for the angle-of-attack case, it can be shown that

$$\left(\Gamma_\xi\right)_\alpha = \left(\Gamma_y\right)_\alpha$$

This simply indicates that in computing span loads the same circulation is used whether one deals with the free stream and the spanwise direction or with the quarter-chord line and the velocity normal to the quarter-chord line. Equation (A13) therefore can be written, per unit length of quarter-chord-line vortex:

$$l_\xi = \rho V_N \left(\Gamma_y\right)_\alpha$$

or, per unit span of the vortex:

$$l_y = \rho \frac{V_N}{\cos \Lambda} \left(\Gamma_y\right)_\alpha \tag{A15}$$

From equation (A14) it can be shown that

$$\left(\Gamma_y\right)_\alpha = \frac{1}{2} Vc\left(c_l\right)_\alpha \tag{A16}$$

Substituting equations (A11) and (A16) into equation (A15) results in

$$l_y = \frac{1}{2} \rho \left[(V - ry) + rx_{c/4} \tan \Lambda\right] V \left(\frac{cc_l}{\bar{c}C_L}\right)_\alpha \bar{c}C_L \tag{A17}$$

per unit span.

The lift of each chordwise-bound vortex must be found through an integration, since the lateral velocity varies along the length of the vortex. The lift is given by

$$l_2 = \int_{x_c}^{x_{c/4}} \rho v \frac{d\left(\Gamma_y\right)_\alpha}{dy} dx$$

or, with substitution of equations (A9) and (A16),

$$l_2 = -\frac{1}{2} \rho r V \bar{c} C_L \int_{x_c}^{x_{c/4}} x \frac{d\left(\frac{cc_l}{\bar{c}C_L}\right)_\alpha}{dy} dx \tag{A18}$$

The local section load coefficient is given by

$$\left(\frac{cc_l}{\bar{c}C_L}\right)_{\alpha,r} = \frac{1}{\bar{c}C_L} \frac{l_y + l_2}{\frac{1}{2}\rho V^2}$$

or using equations (A17) and (A18) and normalizing with respect to the semispan gives

$$\left(\frac{cc_l}{\bar{c}C_L}\right)_{\alpha,r} = \left(1 - \frac{rb}{2V} y^* + \frac{rb}{2V} x^*_{c/4} \tan \Lambda\right) \left(\frac{cc_l}{\bar{c}C_L}\right)_\alpha - \int_{x^*_c}^{x^*_{c/4}} \frac{rb}{2V} x^* \frac{d\left(\frac{cc_l}{\bar{c}C_L}\right)_\alpha}{dy^*} dx^* \tag{A19}$$

APPENDIX A

Since $d\left(\frac{cc_l}{\bar{c}C_L}\right)_\alpha \Big/ dy^*$ is not a function of x, the integral of equation (A19) can be evaluated easily, and equation (A19) becomes

$$\left(\frac{cc_l}{\bar{c}C_L}\right)_{\alpha,r} = \left[1 - \frac{rb}{2V}\left(y^* - x^*_{c/4}\tan\Lambda\right)\right]\left(\frac{cc_l}{\bar{c}C_L}\right)_\alpha - \frac{1}{2}\frac{rb}{2V}\left[\left(x^*_{c/4}\right)^2 - \left(x^*_c\right)^2\right]\frac{d\left(\frac{cc_l}{\bar{c}C_L}\right)_\alpha}{dy^*} \tag{A20}$$

The incremental load parameter due to yawing is given by

$$\left(\frac{cc_l}{\bar{c}C_L\frac{rb}{2V}}\right) = \left(-y^* + x^*_{c/4}\tan\Lambda\right)\left(\frac{cc_l}{\bar{c}C_L}\right)_\alpha - \frac{1}{2}\frac{d\left(\frac{cc_l}{\bar{c}C_L}\right)_\alpha}{dy^*}\left[\left(x^*_{c/4}\right)^2 - \left(x^*_c\right)^2\right] \tag{A21}$$

Similarly, for the left wing semispan,

$$\left(\frac{cc_l}{\bar{c}C_L\frac{rb}{2V}}\right) = \left(-y^* - x^*_{c/4}\tan\Lambda\right)\left(\frac{cc_l}{\bar{c}C_L}\right)_\alpha - \frac{1}{2}\frac{d\left(\frac{cc_l}{\bar{c}C_L}\right)_\alpha}{dy^*}\left[\left(x^*_{c/4}\right)^2 - \left(x^*_c\right)^2\right] \tag{A22}$$

In general, the rolling-moment parameter for a wing is given by

$$\frac{C_l}{C_L} = -\frac{1}{4}\int_{-1}^{1}\left(\frac{cc_l}{\bar{c}C_L}\right)y^*dy^* \tag{A23}$$

The rolling-moment parameter due to yawing is given by

$$\frac{C_{l_r}}{C_L} = -\frac{1}{4}\int_{-1}^{1}\left(\frac{cc_l}{\bar{c}C_L\frac{rb}{2V}}\right)y^*dy^* \tag{A24}$$

Considerations of symmetry and the use of equations (A21) and (A22) with equation (A24) result in

$$\frac{C_{l_r}}{C_L} = \frac{1}{2}\int_0^1\left\{\left(y^* - x^*_{c/4}\tan\Lambda\right)\left(\frac{cc_l}{\bar{c}C_L}\right)_\alpha + \frac{1}{2}\left[\left(x^*_{c/4}\right)^2 - \left(x^*_c\right)^2\right]\frac{d\left(\frac{cc_l}{\bar{c}C_L}\right)_\alpha}{dy^*}\right\}y^*dy^* \tag{A25}$$

Equation (A25) is perfectly general and somewhat complex for an arbitrary wing. If the wing leading and trailing edges are straight, however, some simplification is possible. In this case (see fig. 3),

$$x^*_{c/4} = \left(\bar{y}^* - y^*\right)\tan\Lambda - x^*_{ac}$$

and

$$x^*_c = x^*_{c/4} - \frac{3}{4}c^*$$

Substituting these relations into equation (A25) results in

$$\frac{C_{l_r}}{C_L} = \frac{1}{2}\int_0^1 \left\{ \left[y^*\left(1 + \tan^2\Lambda\right) - \left(\bar{y}^*\tan\Lambda - x^*_{ac}\right)\tan\Lambda \right] \left(\frac{cc_l}{\bar{c}C_L}\right)_\alpha \right.$$

$$\left. + \frac{c^*}{2}\left[\frac{3}{2}\left(\bar{y}^* - y^*\right)\tan\Lambda - \frac{3}{2}x^*_{ac} - \frac{9}{16}c^*\right] \frac{d\left(\frac{cc_l}{\bar{c}C_L}\right)_\alpha}{dy^*} \right\} y^* dy^* \qquad \text{(A26)}$$

Integration of equation (A26) is very lengthy and tedious. The solution of equation (A26) is given by

$$\frac{C_{l_r}}{C_L} = \left[\frac{1}{2}\left(1 + \tan^2\Lambda\right) - \frac{9\tan\Lambda}{2A}\frac{1-\lambda}{1+\lambda} + \frac{27}{4A^2}\left(\frac{1-\lambda}{1+\lambda}\right)^2\right]\left(\tilde{y}^*\right)^2 + \left[\frac{3}{A}\frac{1-\lambda}{1+\lambda}\tan\Lambda - \frac{1}{2}\tan^2\Lambda\right]\left(\bar{y}^*\right)^2$$

$$+ \left[\frac{3\tan\Lambda}{2A(1+\lambda)} - \frac{9(1-\lambda)}{A^2(1+\lambda)^2}\right]\bar{y}^* + \left[\frac{\tan\Lambda}{2} - \frac{3}{A}\frac{1-\lambda}{1+\lambda}\right]x^*_{ac}\bar{y}^* + \frac{3x^*_{ac}}{2A(1+\lambda)} + \frac{9}{4A^2(1+\lambda)^2} \qquad \text{(A27)}$$

Rolling Wing

In the analysis of the rolling wing the additional local angle of attack due to rolling must be considered. This additional local angle gives rise to an incremental circulation and therefore an incremental lift. Thus the net lift at any spanwise position is given by

$$\left(c_l\right)_{\alpha,p} = \left(c_l\right)_\alpha \left[1 + \frac{\left(c_l\right)_p}{\left(c_l\right)_\alpha}\right] \tag{A28}$$

This can also be expressed as

$$\left(c_l\right)_{\alpha,p} = \left(c_l\right)_\alpha \left[1 + \frac{\left(c_{l_\alpha}\right)_p \frac{py}{V}}{\left(c_{l_\alpha}\right)_\alpha \alpha}\right] \tag{A29}$$

where $\left(c_{l_\alpha}\right)_p$ and $\left(c_{l_\alpha}\right)_\alpha$ are the local three-dimensional section lift-curve slopes in rolling flight and at angle of attack, respectively. As a first approximation, it is assumed that the local lift-curve slope is equal to the lift-curve slope of the wing semispan. With this assumption,

$$\left.\begin{aligned} \left(c_{l_\alpha}\right)_\alpha &= C_{L_\alpha} \\ \left(c_{l_\alpha}\right)_p &= \left(C_{L_\alpha}\right)_p \end{aligned}\right\} \tag{A30}$$

The additional lift due to rolling is antisymmetric over the wing; therefore, the effective lift-curve slope of the wing semispan in roll is approximately the lift-curve slope of a wing having the geometry (A and Λ) of the wing semispan. A convenient and accurate expression for wing lift-curve slope in incompressible flow is (from ref. 14)

$$C_{L_\alpha} = \frac{Aa_o}{2 + \left[\left(\frac{A}{\cos \Lambda}\right)^2 + 4\right]^{1/2}} \tag{A31}$$

Therefore, for the wing in roll the lift-curve slope is given approximately by

$$\left(C_{L_\alpha}\right)_p = \frac{\frac{A}{2} a_o}{2 + \left[\left(\frac{A}{2 \cos \Lambda}\right)^2 + 4\right]^{1/2}}$$

or, if a_o assumes its theoretical value of 2π,

$$\left(C_{L_\alpha}\right)_p = \frac{\pi A}{2 + \left[\left(\frac{A}{2\cos\Lambda}\right)^2 + 4\right]^{1/2}} \tag{A32}$$

Using relations (A30), (A31), and (A32) with equation (A29) results in

$$\left(c_l\right)_{\alpha,p} = \left(c_l\right)_\alpha \left\{1 + \frac{\dfrac{\pi A}{2 + \left[\left(\frac{A}{2\cos\Lambda}\right)^2 + 4\right]^{1/2}}}{C_L} \frac{pb}{2V}\, y^*\right\} \tag{A33}$$

Since the lift coefficient given by equation (A33) is all associated with the angle-of-attack type of loading, it can be directly related to circulation through equation (A16), so that

$$\Gamma_y = \frac{1}{2} Vc\left(c_l\right)_\alpha \left\{1 + \frac{\dfrac{\pi A}{2 + \left[\left(\frac{A}{2\cos\Lambda}\right)^2 + 4\right]^{1/2}}}{C_L}\, y^* \frac{pb}{2V}\right\} \tag{A34}$$

It is now necessary to consider forces and moments due to interaction of the velocity components with the vortex system having the circulation distribution given by equation (A34). The velocity components are the rectilinear velocity V and the velocity (normal to the wing plane) py.

The interaction of the velocity V with the quarter-chord-line vortex results in a wing rolling moment given by

$$M_X = -\int_{-b/2}^{b/2} \rho V \Gamma_y y \, dy \tag{A35}$$

or using equation (A34), nondimensionalizing, and taking the derivative with respect to $pb/2V$ gives

$$C_{l_p} = -\frac{\frac{\pi A}{2}}{2 + \left[\left(\frac{A}{2\cos\Lambda}\right)^2 + 4\right]^{1/2}} \int_0^1 \left(\frac{cc_l}{\bar{c}C_L}\right)_\alpha (y^*)^2 dy^*$$

From the definition of $\tilde{y}^*$ in equation (1), it is seen that

$$C_{l_p} = -\frac{1}{2} \frac{\pi A}{2 + \left[\left(\frac{A}{2\cos\Lambda}\right)^2 + 4\right]^{1/2}} (\tilde{y}^*)^2 \tag{A36}$$

Next the interaction of the rolling velocity py with the vortex system is considered. This velocity is normal to the wing vortex plane. Since flow through the vortex sheet is not permitted, only the interaction of the additional velocity py with the quarter-chord-line vortex and the extreme wing-tip chordwise-bound vortices need be considered.

The force caused by interaction of py with a chordwise-bound vortex is given by

$$(f_Y)_1 = \frac{3}{4} c\rho py \frac{d\Gamma_y}{dy} dy$$

or, with substitution from equation (A16),

$$(f_Y)_1 = \frac{3}{8} \rho py V \bar{c} c C_L \frac{d\left(\frac{cc_l}{\bar{c}C_L}\right)_\alpha}{dy} dy$$

This force is in the wing (or vortex) plane and is in the y-direction (perpendicular to the chordwise-bound vortices). One approach to evaluating this force for the wing-tip vortices is to perform the integration

$$\Delta(f_Y)_1 = 2 \int_{(b/2)-\epsilon}^{b/2} \frac{3}{8} \rho c py V \bar{c} C_L \frac{d\left(\frac{cc_l}{\bar{c}C_L}\right)_\alpha}{dy} dy$$

or

$$\Delta\left(f_Y\right)_1 = \frac{3}{4}\rho p V \bar{c} C_L \int_{\left[\left(\frac{cc_l}{\bar{c}C_L}\right)_\alpha\right]_{(b/2)-\epsilon}}^{\left[\left(\frac{cc_l}{\bar{c}C_L}\right)_\alpha\right]_{b/2}} yc\, d\left(\frac{cc_l}{\bar{c}C_L}\right)_\alpha$$

This equation can be evaluated by parts, with the result

$$\Delta\left(f_Y\right)_1 = \frac{3}{4}\rho p V \bar{c} C_L \left\{ yc\left(\frac{cc_l}{\bar{c}C_L}\right)_\alpha \Bigg|_{\left[\left(\frac{cc_l}{\bar{c}C_L}\right)_\alpha\right]_{(b/2)-\epsilon}}^{\left[\left(\frac{cc_l}{\bar{c}C_L}\right)_\alpha\right]_{b/2}} - \int_{(b/2)-\epsilon}^{b/2} \left(\frac{cc_l}{\bar{c}C_L}\right)_\alpha \left(c + y\frac{dc}{dy}\right) dy \right\}$$

Since all the functions involved in this equation are regular and well-behaved in the indicated limits, it is apparent that $\Delta\left(f_Y\right)_1$ will approach zero as ϵ approaches zero. Therefore, from the analysis made in this paper, the wing-tip vortices will contribute no resultant force or moment due to rolling velocity – that is, $\Delta\left(f_Y\right)_1 = 0$.

The next possibility to consider is the interaction of the rolling-velocity components with the circulation on the quarter-chord line. The associated force is in the wing plane and is perpendicular to the quarter-chord line. The magnitude of the force is

$$\left(f_Y\right)_2 = \rho p y \Gamma_y \tag{A37}$$

per unit of vortex length. This force results in a side force which can be written as

$$F_Y = V\rho \frac{pb}{2V} y^* \Gamma_y \tan \Lambda \tag{A38}$$

per unit of span. A resulting side-force coefficient is given by

$$C_Y = \int_{-b/2}^{b/2} \frac{F_Y}{\frac{1}{2}\rho V^2 S}\, dy \tag{A39}$$

Using equations (A34) and (A38) with (A39) and retaining up to first-order terms in $pb/2V$ results in

APPENDIX A

$$C_Y = \int_0^1 C_L \left(\frac{cc_l}{\bar{c}C_L}\right)_\alpha \frac{pb}{2V} y^* \tan \Lambda \, dy^*$$

The coefficient of side force due to rolling is found to be

$$\frac{C_{Y_p}}{C_L} = \tan \Lambda \int_0^1 \left(\frac{cc_l}{\bar{c}C_L}\right)_\alpha y^* dy^*$$

which integrates to

$$\frac{C_{Y_p}}{C_L} = \bar{y}^* \tan \Lambda \tag{A40}$$

The force given by equation (A37) also results in a yawing moment which is given by

$$M_Z = \int_{-b/2}^{b/2} \left(x_{c/4} \sin \Lambda - y \cos \Lambda\right) \frac{(f_Y)_2}{\cos \Lambda} dy$$

or, proceeding as before to form the yawing-moment coefficient,

$$\frac{C_{n_p}}{C_L} = \frac{1}{2} \int_0^1 \left(\frac{cc_l}{\bar{c}C_L}\right)_\alpha \left(x^*_{c/4} \tan \Lambda - y^*\right) y^* dy^*$$

Integration of this equation results in

$$\frac{C_{n_p}}{C_L} = -\frac{1}{2}\left\{\left(\tilde{y}^*\right)^2 + \left[\left(\tilde{y}^*\right)^2 - \left(\bar{y}^*\right)^2\right] \tan^2 \Lambda + x^*_{ac} \bar{y}^* \tan \Lambda\right\} \tag{A41}$$

APPENDIX B

COMPRESSIBILITY EFFECTS

The effects of compressibility on the span loads and derivatives can be estimated by proper treatment of the local span load. As a first approximation, the load coefficient at a particular spanwise position is assumed to increase in direct proportion to the total wing lift coefficient. At a constant angle of attack, therefore,

$$\frac{(c_l)_M}{(c_l)_{M=0}} = \frac{(C_L)_M}{(C_L)_{M=0}} = \frac{(C_{L_\alpha})_M}{(C_{L_\alpha})_{M=0}} \tag{B1}$$

Note that this assumption indicates no effect of compressibility on the center of pressure of the span load.

A convenient equation for wing lift-curve slope, given in reference 14, is

$$C_{L_\alpha} = \frac{\dfrac{Aa_o}{\left(1 - M_N^2\right)^{1/2}}}{\dfrac{a_o}{\pi\left(1 - M_N^2\right)^{1/2}} + \left[\left(\dfrac{A}{\cos \Lambda}\right)^2 + \dfrac{a_o^2}{\pi^2\left(1 - M_N^2\right)}\right]^{1/2}} \tag{B2}$$

Combining equations (B1) and (B2) and letting a_o assume its theoretical value of 2π results in

$$\frac{(c_l)_M}{(c_l)_{M=0}} = \frac{2 + \left[\left(\dfrac{A}{\cos \Lambda}\right)^2 + 4\right]^{1/2}}{2 + \left[\left(\dfrac{A}{\cos \Lambda}\right)^2 \left(1 - M_N^2\right) + 4\right]^{1/2}} \tag{B3}$$

Equation (B3) can be used to modify the local span load and resulting derivatives to account for Mach number effects.

Sideslipping Wing

Reference 17 shows that for a sideslipping wing at an angle of attack in incompressible flow the local span-load parameter is given by

$$\left(\frac{cc_l}{\bar{c}}\right)_{\beta,\alpha} = \left(\frac{cc_l}{\bar{c}}\right)_{\alpha}(1 + \beta \tan \Lambda) - \frac{3}{4} c^*\beta \frac{d\left(\frac{cc_l}{\bar{c}}\right)_{\alpha}}{dy^*} \tag{B4}$$

The Mach number perpendicular to the wing quarter-chord line is given by

$$M_N = M \cos(\Lambda - \beta) \tag{B5}$$

Combining equations (B3), (B4), and (B5) results in

$$\left(\frac{cc_l}{\bar{c}}\right)_{M,\beta,\alpha} = \frac{2 + \left[\left(\frac{A}{\cos \Lambda}\right)^2 + 4\right]^{1/2}}{2 + \left\{\left(\frac{A}{\cos \Lambda}\right)^2\left[1 - M^2\cos^2(\Lambda - \beta)\right] + 4\right\}^{1/2}}\left[\left(\frac{cc_l}{\bar{c}}\right)_{\alpha}(1 + \beta \tan \Lambda) - \frac{3}{4} c^*\beta \frac{d\left(\frac{cc_l}{\bar{c}}\right)_{\alpha}}{dy^*}\right] \tag{B6}$$

The span-load increment due to sideslip is found by differentiating equation (B6) with respect to β and ignoring higher order terms in β (letting β approach zero). The result is

$$\left(\frac{cc_l}{\bar{c}\beta}\right)_M = \frac{2 + \left[\left(\frac{A}{\cos \Lambda}\right)^2 + 4\right]^{1/2}}{2 + \left[\left(\frac{A}{\cos \Lambda}\right)^2\left(1 - M^2\cos^2\Lambda\right) + 4\right]^{1/2}}\left[\left(\frac{cc_l}{\bar{c}}\right)_{\alpha} \tan \Lambda - \frac{3}{4} c^* \frac{d\left(\frac{cc_l}{\bar{c}}\right)_{\alpha}}{dy^*}\right]$$

$$+ \frac{\left(\frac{cc_l}{\bar{c}}\right)_{\alpha} A^2M^2(\tan \Lambda)\left\{2 + \left[\left(\frac{A}{\cos \Lambda}\right)^2 + 4\right]^{1/2}\right\}}{\left[\left(\frac{A}{\cos \Lambda}\right)^2\left(1 - M^2\cos^2\Lambda\right) + 4\right]^{1/2}\left\{2 + \left[\left(\frac{A}{\cos \Lambda}\right)^2\left(1 - M^2\cos^2\Lambda\right) + 4\right]^{1/2}\right\}^2} \tag{B7}$$

It should be noted that for zero sideslip, equation (B3) reduces to

$$\frac{\left(c_l\right)_{M,\alpha}}{\left(c_l\right)_{\alpha}} = \frac{2 + \left[\left(\frac{A}{\cos \Lambda}\right)^2 + 4\right]^{1/2}}{2 + \left[\left(\frac{A}{\cos \Lambda}\right)^2 \left(1 - M^2 \cos^2 \Lambda\right) + 4\right]^{1/2}} \tag{B8}$$

Using relation (B8) with equation (B7) and dividing through by total lift coefficient results in

$$\left(\frac{cc_l}{\bar{c}C_{L_\beta}}\right)_M = \left(\frac{cc_l}{\bar{c}C_L}\right)_{M,\alpha} \tan \Lambda - \frac{3}{4} c^* \frac{d\left(\frac{cc_l}{\bar{c}C_L}\right)_{M,\alpha}}{dy^*} + \left(\frac{cc_l}{\bar{c}C_L}\right)_{M,\alpha} \frac{A^2 M^2 \tan \Lambda}{\left[\left(\frac{A}{\cos \Lambda}\right)^2 - A^2M^2 + 4\right]^{1/2} \left\{2 + \left[\left(\frac{A}{\cos \Lambda}\right)^2 - A^2M^2 + 4\right]^{1/2}\right\}} \tag{B9}$$

The rolling-moment parameter due to sideslip is (from ref. 17)

$$\frac{C_{l_\beta}}{C_L} = -\frac{1}{2} \int_0^1 \left(\frac{cc_l}{\bar{c}C_{L_\beta}}\right) y^* dy^* + 0.05$$

or, using equation (B9),

$$\left(\frac{C_{l_\beta}}{C_L}\right)_M = -\frac{1}{2} \int_0^1 \left[\left(\frac{cc_l}{\bar{c}C_L}\right)_{M,\alpha} \tan \Lambda - \frac{3}{4} c^* \frac{d\left(\frac{cc_l}{\bar{c}C_L}\right)_{M,\alpha}}{dy^*}\right] y^* dy^* + 0.05$$

$$-\frac{1}{2} \int_0^1 \left(\frac{cc_l}{\bar{c}C_L}\right)_{M,\alpha} \frac{A^2 M^2 \tan \Lambda}{\left[\left(\frac{A}{\cos \Lambda}\right)^2 - A^2M^2 + 4\right]^{1/2} \left\{2 + \left[\left(\frac{A}{\cos \Lambda}\right)^2 - A^2M^2 + 4\right]^{1/2}\right\}} y^* dy^* \tag{B10}$$

The correction factor 0.05, as discussed in reference 17, is independent of aspect ratio or sweep angle. Since compressibility effects can be related to geometric changes by the Prandtl-Glauert relations, and since geometry has no effect on the factor 0.05, it would appear that the factor is not a function of Mach number.

Performing the integration as was done for the incompressible-flow case yields (for a trapezoidal wing)

$$\left(\frac{C_{l_\beta}}{C_L}\right)_M = -\frac{1}{2}\left[\frac{3}{A(1+\lambda)} + \bar{y}^*\left(\tan\Lambda - \frac{6}{A}\frac{1-\lambda}{1+\lambda}\right)\right] + 0.05 - \frac{1}{2}\bar{y}^* \frac{A^2M^2\tan\Lambda}{\left[\left(\frac{A}{\cos\Lambda}\right)^2 - A^2M^2 + 4\right]^{1/2}\left\{2 + \left[\left(\frac{A}{\cos\Lambda}\right)^2 - A^2M^2 + 4\right]^{1/2}\right\}} \tag{B11}$$

Comparison of this equation with equation (A6) shows that

$$\left(\frac{C_{l_\beta}}{C_L}\right)_M = \left(\frac{C_{l_\beta}}{C_L}\right)_{M=0} - \frac{1}{2}\bar{y}^* \frac{A^2M^2\tan\Lambda}{\left[\left(\frac{A}{\cos\Lambda}\right)^2 - A^2M^2 + 4\right]^{1/2}\left\{2 + \left[\left(\frac{A}{\cos\Lambda}\right)^2 - A^2M^2 + 4\right]^{1/2}\right\}}$$

Yawing Wing

The span load for a yawing wing in compressible flow can be determined in a manner analogous to that for the sideslip case. In yawing flight, however, the effective Mach number varies across the wing span. The velocity normal to the wing quarter-chord line is given by equation (A11), and the corresponding Mach number is

$$M_N = M\left[\cos\Lambda - \frac{rb}{2V}\left(y^*\cos\Lambda - x^*_{c/4}\sin\Lambda\right)\right] \tag{B12}$$

Using equations (B3) and (B12) with equation (A20) results in

$$\left(\frac{cc_l}{\bar{c}C_L}\right)_{M,r,\alpha} = \frac{\left\{2 + \left[\left(\frac{A}{\cos\Lambda}\right)^2 + 4\right]^{1/2}\right\}\left\{\left[1 - \frac{rb}{2V}\left(y^* - x^*_{c/4}\tan\Lambda\right)\right]\left(\frac{cc_l}{\bar{c}C_L}\right)_\alpha - \frac{1}{2}\frac{rb}{2V}\left[\left(x^*_{c/4}\right)^2 - \left(x^*_c\right)^2\right]\frac{d\left(\frac{cc_l}{\bar{c}C_L}\right)_\alpha}{dy^*}\right\}}{2 + \left\{\frac{A^2}{\cos^2\Lambda} - \frac{A^2}{\cos^2\Lambda}M^2\left[\cos\Lambda - \frac{rb}{2V}\left(y^*\cos\Lambda - x^*_{c/4}\sin\Lambda\right)\right]^2 + 4\right\}^{1/2}} \tag{B13}$$

Differentiating equation (B13) with respect to rb/2V, letting rb/2V approach zero, and proceeding as in the sideslip case, results in the following span-load parameter:

$$\left(\frac{cc_l}{\bar{c}C_L\frac{rb}{2V}}\right)_M = \left(-y^* + x^*_{c/4}\tan\Lambda\right)\left(\frac{cc_l}{\bar{c}C_L}\right)_{M,\alpha} - \frac{1}{2}\left[\left(x^*_{c/4}\right)^2 - \left(x^*_c\right)^2\right]\frac{d\left(\frac{cc_l}{\bar{c}C_L}\right)_{M,\alpha}}{dy^*}$$

$$+ \left(\frac{cc_l}{\bar{c}C_L}\right)_{M,\alpha}\frac{A^2M^2\left(-y^* + x^*_{c/4}\tan\Lambda\right)}{\left[\left(\frac{A}{\cos\Lambda}\right)^2 - A^2M^2 + 4\right]^{1/2}\left\{2 + \left[\left(\frac{A}{\cos\Lambda}\right)^2 - A^2M^2 + 4\right]^{1/2}\right\}} \tag{B14}$$

The rolling-moment parameter due to yawing is found by substituting equation (B14) into equation (A24) and performing the integrations in the same manner as was done in the incompressible case. The result is found to be

$$\left(\frac{C_{l_r}}{C_L}\right)_M = \left[\frac{1}{2}\left(1 + \tan^2\Lambda\right) - \frac{9\tan\Lambda}{2A}\frac{1-\lambda}{1+\lambda} + \frac{27}{4A^2}\left(\frac{1-\lambda}{1+\lambda}\right)^2\right]\left(\tilde{y}^*\right)^2 + \left(\frac{3}{A}\frac{1-\lambda}{1+\lambda}\tan\Lambda - \frac{1}{2}\tan^2\Lambda\right)\left(\bar{y}^*\right)^2$$

$$+\left[\frac{3\tan\Lambda}{2A(1+\lambda)} - \frac{9(1-\lambda)}{A^2(1+\lambda)^2}\right]\bar{y}^* + \left(\frac{\tan\Lambda}{2} - \frac{3}{A}\frac{1-\lambda}{1+\lambda}\right)x^*_{ac}\bar{y}^* + \frac{3x^*_{ac}}{2A(1+\lambda)} + \frac{9}{4A^2(1+\lambda)^2}$$

$$+\frac{A^2M^2}{2}\frac{-\left(\bar{y}^*\right)^2\tan^2\Lambda + \left(\tilde{y}^*\right)^2\left(1+\tan^2\Lambda\right) + x^*_{ac}\bar{y}^*\tan\Lambda}{\left[\left(\frac{A}{\cos\Lambda}\right)^2 - A^2M^2 + 4\right]^{1/2}\left\{2 + \left[\left(\frac{A}{\cos\Lambda}\right)^2 - A^2M^2 + 4\right]^{1/2}\right\}}$$

Comparison of this equation with equation (A27) shows that

$$\left(\frac{C_{l_r}}{C_L}\right)_M = \left(\frac{C_{l_r}}{C_L}\right)_{M=0} + \frac{A^2M^2}{2}\frac{-\left(\bar{y}^*\right)^2\tan^2\Lambda + \left(\tilde{y}^*\right)^2\left(1+\tan^2\Lambda\right) + x^*_{ac}\bar{y}^*\tan\Lambda}{\left[\left(\frac{A}{\cos\Lambda}\right)^2 - A^2M^2 + 4\right]^{1/2}\left\{2 + \left[\left(\frac{A}{\cos\Lambda}\right)^2 - A^2M^2 + 4\right]^{1/2}\right\}} \qquad \text{(B15)}$$

Rolling Wing

In compressible flow, equation (A28) becomes

$$\left(c_l\right)_{M,\alpha,p} = \left(c_l\right)_{M,\alpha}\left[1 + \frac{\left(c_l\right)_{M,p}}{\left(c_l\right)_{M,\alpha}}\right] \qquad \text{(B16)}$$

APPENDIX B

The compressibility correction to $\left(c_l\right)_{M,p}$ is based on the aspect ratio of a wing semi-span, as discussed previously; therefore, from equation (B2),

$$\left(C_{L_\alpha}\right)_{M,p} = \frac{\pi A}{2 + \left[\left(\frac{A}{2 \cos \Lambda}\right)^2 \left(1 - M_N^2\right) + 4\right]^{1/2}}$$

and

$$\left(c_l\right)_{M,p} = \frac{\pi A \frac{pb}{2V} y^*}{2 + \left[\left(\frac{A}{2 \cos \Lambda}\right)^2 \left(1 - M_N^2\right) + 4\right]^{1/2}} \tag{B17}$$

It can be shown that equation (B16) becomes

$$\left(c_l\right)_{M,p,\alpha} = \left(c_l\right)_{M,\alpha} \left\{ 1 + \frac{\frac{\pi A}{2 + \left[\left(\frac{A}{2 \cos \Lambda}\right)^2 \left(1 - M_N^2\right) + 4\right]^{1/2}} \frac{pb}{2V} y^*}{\left(C_L\right)_M} \right\} \tag{B18}$$

In rolling flow the velocity perpendicular to the wing quarter-chord line is given by

$$V_N = \left[(V \cos \Lambda)^2 + V^2 \left(\frac{pb}{2V}\right)^2 (y^*)^2\right]^{1/2}$$

and the corresponding Mach number is

$$M_N = M\left[\cos^2 \Lambda + \left(\frac{pb}{2V}\right)^2 (y^*)^2\right]^{1/2} \tag{B19}$$

Substituting equation (B19) into (B18), differentiating with respect to pb/2V, and letting pb/2V approach zero results in the span-load parameter

$$\left(\frac{cc_l}{\bar{c} \frac{pb}{2V}}\right)_M = \left(\frac{cc_l}{\bar{c} C_L}\right)_{M,\alpha} \frac{\pi A y^*}{2 + \left[\frac{1}{4}\left(\frac{A}{\cos \Lambda}\right)^2 - \frac{A^2 M^2}{4} + 4\right]^{1/2}}$$

APPENDIX B

The circulation for the rolling wing in compressible flow is found by use of equations (A16), (B18), and (B19), and is

$$\left(\Gamma_y\right)_{M,p,\alpha} = \frac{1}{2} Vc\left(c_l\right)_{M,\alpha}\left[1 + \frac{\dfrac{\pi A}{2 + \left\{\left(\dfrac{A}{2\cos\Lambda}\right)^2\left[1 - M^2\cos^2\Lambda - M^2\left(\dfrac{pb}{2V}\right)^2\left(y^*\right)^2\right] + 4\right\}^{1/2}}\dfrac{pb}{2V}y^*}{\left(C_L\right)_M}\right] \tag{B20}$$

Substitution of equation (B20) into (A35), nondimensionalizing, taking the derivative with respect to pb/2V, and letting pb/2V approach zero results in the rolling-moment parameter

$$C_{l_p} = -\frac{1}{2}\int_0^1 \left(\frac{cc_l}{\bar{c}C_L}\right)_{M,\alpha} \frac{\pi A}{2 + \left[\dfrac{1}{4}\left(\dfrac{A}{\cos\Lambda}\right)^2 - \dfrac{A^2M^2}{4} + 4\right]^{1/2}}\left(y^*\right)^2 dy^* \tag{B21}$$

Performing the integration results in

$$C_{l_p} = -\frac{1}{2}\frac{\pi A}{2 + \left[\dfrac{1}{4}\left(\dfrac{A}{\cos\Lambda}\right)^2 - \dfrac{A^2M^2}{4} + 4\right]^{1/2}}\left(\tilde{y}^*\right)^2 \tag{B22}$$

Comparison of equations (A36) and (B22) shows that

$$\left(C_{l_p}\right)_M = \left(C_{l_p}\right)_{M=0}\frac{2 + \left[\left(\dfrac{A}{2\cos\Lambda}\right)^2 + 4\right]^{1/2}}{2 + \left[\dfrac{1}{4}\left(\dfrac{A}{\cos\Lambda}\right)^2 - \dfrac{A^2M^2}{4} + 4\right]^{1/2}} \tag{B23}$$

The side force due to rolling is found through use of equations (A38), (A39), and (B20), and is (for pb/2V approaching zero)

$$\frac{C_{Y_p}}{C_L} = \bar{y}^*\tan\Lambda \tag{B24}$$

APPENDIX B

Comparison of equations (B24) and (A40) indicates that there is no compressibility effect on the parameter C_{Y_p}/C_L. Similarly, it can be shown that there is no compressibility effect on the parameter C_{n_p}/C_L.

APPENDIX C

SUMMARY OF EQUATIONS

General Equations for Additional Local Span Loading

Sideslipping wing:

$$\left(\frac{cc_l}{\bar{c}C_{L\beta}}\right)_M = \left(\frac{cc_l}{\bar{c}C_L}\right)_{M,\alpha} \tan\Lambda - \frac{3}{4}c^* \frac{d\left(\frac{cc_l}{\bar{c}C_L}\right)_{M,\alpha}}{dy^*} + \left(\frac{cc_l}{\bar{c}C_L}\right)_{M,\alpha} \frac{A^2M^2\tan\Lambda}{\left[\left(\frac{A}{\cos\Lambda}\right)^2 - A^2M^2 + 4\right]^{1/2}\left\{2 + \left[\left(\frac{A}{\cos\Lambda}\right)^2 - A^2M^2 + 4\right]^{1/2}\right\}} \tag{C1}$$

Yawing wing:

$$\left(\frac{cc_l}{\bar{c}C_L\frac{rb}{2V}}\right)_M = \left(-y^* + x^*_{c/4}\tan\Lambda\right)\left(\frac{cc_l}{\bar{c}C_L}\right)_{M,\alpha} - \frac{1}{2}\left[\left(x^*_{c/4}\right)^2 - \left(x^*_c\right)^2\right]\frac{d\left(\frac{cc_l}{\bar{c}C_L}\right)_{M,\alpha}}{dy^*}$$

$$+ \left(\frac{cc_l}{\bar{c}C_L}\right)_{M,\alpha} \frac{A^2M^2\left(-y^* + x^*_{c/4}\tan\Lambda\right)}{\left[\left(\frac{A}{\cos\Lambda}\right)^2 - A^2M^2 + 4\right]^{1/2}\left\{2 + \left[\left(\frac{A}{\cos\Lambda}\right)^2 - A^2M^2 + 4\right]^{1/2}\right\}} \tag{C2}$$

Rolling wing:

$$\left(\frac{cc_l}{\bar{c}\frac{pb}{2V}}\right)_{M,\alpha} = \left(\frac{cc_l}{\bar{c}C_L}\right)_{M,\alpha} \frac{\pi A y^*}{2 + \left[\frac{1}{4}\left(\frac{A}{\cos\Lambda}\right)^2 - \frac{A^2M^2}{4} + 4\right]^{1/2}} \tag{C3}$$

Sideslipping wing:

$$\left(\frac{cc_l}{\bar{c}C_{L\beta}}\right)_M = \left(\frac{cc_l}{\bar{c}C_L}\right)_{M,\alpha} \tan\Lambda - \frac{3}{A(1+\lambda)}\left[1-(1-\lambda)y^*\right]\frac{d\left(\frac{cc_l}{\bar{c}C_L}\right)_{M,\alpha}}{dy^*} + \left(\frac{cc_l}{\bar{c}C_L}\right)_{M,\alpha} \frac{A^2M^2\tan\Lambda}{\left[\left(\frac{A}{\cos\Lambda}\right)^2 - A^2M^2 + 4\right]^{1/2}\left\{2+\left[\left(\frac{A}{\cos\Lambda}\right)^2 - A^2M^2 + 4\right]^{1/2}\right\}} \tag{C4}$$

Yawing wing:

$$\left(\frac{cc_l}{\bar{c}C_L\frac{rb}{2V}}\right)_M = -\left\{y^* - \left[\left(\bar{y}^* - y^*\right)\tan\Lambda - x^*_{ac}\right]\tan\Lambda\right\}\left(\frac{cc_l}{\bar{c}C_L}\right)_{M,\alpha} - \frac{2}{A(1+\lambda)}\left[1-(1-\lambda)y^*\right]\left\{\frac{3}{2}\left(\bar{y}^* - y^*\right)\tan\Lambda - \frac{3}{2}x^*_{ac} - \frac{9}{4A(1+\lambda)}\left[1-(1-\lambda)y^*\right]\right\}\frac{d\left(\frac{cc_l}{\bar{c}C_L}\right)_{M,\alpha}}{dy^*} + \left(\frac{cc_l}{\bar{c}C_L}\right)_{M,\alpha} \frac{-A^2M^2\left\{y^* - \left[\left(\bar{y}^* - y^*\right)\tan\Lambda - x^*_{ac}\right]\tan\Lambda\right\}}{\left[\left(\frac{A}{\cos\Lambda}\right)^2 - A^2M^2 + 4\right]^{1/2}\left\{2+\left[\left(\frac{A}{\cos\Lambda}\right)^2 - A^2M^2 + 4\right]^{1/2}\right\}} \tag{C5}$$

Rolling wing:

$$\left(\frac{cc_l}{\bar{c}\frac{pb}{2V}}\right)_M = \left(\frac{cc_l}{\bar{c}C_L}\right)_{M,\alpha} y^* \frac{\pi A}{2+\left[\frac{1}{4}\left(\frac{A}{\cos\Lambda}\right)^2 - \frac{A^2M^2}{4} + 4\right]^{1/2}} \tag{C6}$$

Sideslipping wing:

$$\left(\frac{C_{l_\beta}}{C_L}\right)_M = -\frac{1}{2}\int_0^1 \left[\left(\frac{cc_l}{\bar{c}C_L}\right)_{M,\alpha} \tan\Lambda - \frac{3}{4}c^* \frac{d\left(\frac{cc_l}{\bar{c}C_L}\right)_{M,\alpha}}{dy^*}\right] y^*dy^* + 0.05 - \frac{1}{2}\int_0^1 \left(\frac{cc_l}{\bar{c}C_L}\right)_{M,\alpha} \frac{A^2M^2\tan\Lambda}{\left[\left(\frac{A}{\cos\Lambda}\right)^2 - A^2M^2 + 4\right]^{1/2}\left\{2 + \left[\left(\frac{A}{\cos\Lambda}\right)^2 - A^2M^2 + 4\right]^{1/2}\right\}} y^*dy^* \tag{C7}$$

Yawing wing:

$$\left(\frac{C_{l_r}}{C_L}\right)_M = \frac{1}{2}\int_0^1 \left\{\left(y^* - x^*_{c/4}\tan\Lambda\right)\left(\frac{cc_l}{\bar{c}C_L}\right)_{M,\alpha} + \frac{1}{2}\left[\left(x^*_{c/4}\right)^2 - \left(x^*_c\right)^2\right]\frac{d\left(\frac{cc_l}{\bar{c}C_L}\right)_{M,\alpha}}{dy^*}\right\} y^*dy^*$$

$$+\frac{1}{2}\int_0^1 \left(\frac{cc_l}{\bar{c}C_L}\right)_{M,\alpha} A^2M^2 \frac{y^* - x^*_{c/4}\tan\Lambda}{\left[\left(\frac{A}{\cos\Lambda}\right)^2 - A^2M^2 + 4\right]^{1/2}\left\{2 + \left[\left(\frac{A}{\cos\Lambda}\right)^2 - A^2M^2 + 4\right]^{1/2}\right\}} y^*dy^* \tag{C8}$$

Rolling wing:

$$\left(C_{l_p}\right)_M = -\frac{1}{2}\frac{\pi A}{2 + \left[\frac{1}{4}\left(\frac{A}{\cos\Lambda}\right)^2 - \frac{A^2M^2}{4} + 4\right]^{1/2}}\int_0^1 \left(\frac{cc_l}{\bar{c}C_L}\right)_{M,\alpha} \left(y^*\right)^2 dy^* \tag{C9}$$

$$\frac{C_{Y_p}}{C_L} = \int_0^1 \left(\frac{cc_l}{\bar{c}C_L}\right)_{M,\alpha} \tan\Lambda y^*dy^* \tag{C10}$$

$$\frac{C_{n_p}}{C_L} = \frac{1}{2}\int_0^1 \left(\frac{cc_l}{\bar{c}C_L}\right)_{M,\alpha}\left(x^*_{c/4}\tan\Lambda - y^*\right) y^*dy^* \tag{C11}$$

Sideslipping wing:

$$\frac{C_{l_\beta}}{C_L} = -\frac{1}{2}\left[\frac{3}{A(1+\lambda)} + \bar{y}^*\left(\tan\Lambda - \frac{6}{A}\frac{1-\lambda}{1+\lambda}\right)\right] + 0.05 - \frac{1}{2}\bar{y}^*\frac{A^2M^2\tan\Lambda}{\left[\left(\frac{A}{\cos\Lambda}\right)^2 - A^2M^2 + 4\right]^{1/2}\left\{2 + \left[\left(\frac{A}{\cos\Lambda}\right)^2 - A^2M^2 + 4\right]^{1/2}\right\}} \tag{C12}$$

Yawing wing:

$$\frac{C_{l_r}}{C_L} = \left[\frac{1}{2}\left(1 + \tan^2\Lambda\right) - \frac{9}{2A}\frac{1-\lambda}{1+\lambda}\tan\Lambda + \frac{27}{4A^2}\left(\frac{1-\lambda}{1+\lambda}\right)^2\right](\tilde{y}^*)^2$$

$$+ \left(\frac{3}{A}\frac{1-\lambda}{1+\lambda}\tan\Lambda - \frac{\tan^2\Lambda}{2}\right)(\bar{y}^*)^2 + \left[\frac{3\tan\Lambda}{2A(1+\lambda)} - \frac{9(1-\lambda)}{A^2(1+\lambda)^2}\right]\bar{y}^* + \left(\frac{\tan\Lambda}{2} - \frac{3}{A}\frac{1-\lambda}{1+\lambda}\right)x_{ac}^*\bar{y}^*$$

$$+ \frac{3x_{ac}^*}{2A(1+\lambda)} + \frac{9}{4A^2(1+\lambda)^2} + \frac{A^2M^2}{2}\frac{-(\bar{y}^*)^2\tan^2\Lambda + (\tilde{y}^*)^2\left(1 + \tan^2\Lambda\right) + x_{ac}^*\bar{y}^*\tan\Lambda}{\left[\left(\frac{A}{\cos\Lambda}\right)^2 - A^2M^2 + 4\right]^{1/2}\left\{2 + \left[\left(\frac{A}{\cos\Lambda}\right)^2 - A^2M^2 + 4\right]^{1/2}\right\}} \tag{C13}$$

Rolling wing:

$$C_{l_p} = -\frac{1}{2}\left(\tilde{y}^*\right)^2 \frac{\pi A}{2 + \left[\left(\frac{A}{2\cos\Lambda}\right)^2 - \frac{A^2M^2}{4} + 4\right]^{1/2}} \tag{C14}$$

$$\frac{C_{Y_p}}{C_L} = \bar{y}^* \tan\Lambda \tag{C15}$$

$$\frac{C_{n_p}}{C_L} = -\frac{1}{2}\left\{\left(\tilde{y}^*\right)^2 + \left[\left(\tilde{y}^*\right)^2 - \left(\bar{y}^*\right)^2\right]\tan^2\Lambda + x^*_{ac}\bar{y}^*\tan\Lambda\right\} \tag{C16}$$

REFERENCES

1. Jones, Arthur L.; and Alksne, Alberta: A Summary of Lateral-Stability Derivatives Calculated for Wing Plan Forms in Supersonic Flow. NACA Rep. 1052, 1951.

2. Margolis, Kenneth: Theoretical Lift and Damping in Roll of Thin Sweptback Tapered Wings With Raked-In and Cross-Stream Wing Tips at Supersonic Speeds. Subsonic Leading Edges. NACA TN 2048, 1950.

3. Harmon, Sidney M.: Stability Derivatives at Supersonic Speeds of Thin Rectangular Wings With Diagonals Ahead of Tip Mach Lines. NACA Rep. 925, 1949. (Supersedes NACA TN 1706.)

4. Ribner, Herbert S.: The Stability Derivatives of Low-Aspect-Ratio Triangular Wings at Subsonic and Supersonic Speeds. NACA TN 1423, 1947.

5. Pearson, Henry A.; and Jones, Robert T.: Theoretical Stability and Control Characteristics of Wings With Various Amounts of Taper and Twist. NACA Rep. 635, 1938.

6. Weissinger, J.: Der schiebende Tragflügel bei gesunder Strömung. Bericht S 2 der Lilienthal-Gesellschaft für Luftfahrtforschung, 1938-1939, pp. 13-51.

7. Multhopp, H.: Methods for Calculating the Lift Distribution of Wings (Subsonic Lifting-Surface Theory). R. & M. No. 2884, Brit. A.R.C., Jan. 1950.

8. DeYoung, John: Theoretical Antisymmetric Span Loading for Wings of Arbitrary Plan Form at Subsonic Speeds. NACA Rep. 1056, 1951. (Supersedes NACA TN 2140.)

9. Falkner, V. M.: The Calculation of Aerodynamic Loading on Surfaces of Any Shape. R. & M. No. 1910, British A.R.C., Aug. 1943.

10. Simpson, Robert W.: An Extension of Multhopp's Lifting Surface Theory to Include the Effect of Flaps, Ailerons, etc., Rep. No. 132, Coll. of Aeronaut., Cranfield (Engl.), May 1960.

11. Weissinger, J.: The Lift Distribution of Swept-Back Wings. NACA TM 1120, 1947.

12. Toll, Thomas A.; and Queijo, M. J.: Approximate Relations and Charts for Low-Speed Stability Derivatives of Swept Wings. NACA TN 1581, 1948.

13. Queijo, M. J.; and Jaquet, Byron M.: Calculated Effects of Geometric Dihedral on the Low-Speed Rolling Derivatives of Swept Wings. NACA TN 1732, 1948.

14. Polhamus, Edward C.; and Sleeman, William C., Jr.: The Rolling Moment Due to Sideslip of Swept Wings at Subsonic and Transonic Speeds. NASA TN D-209, 1960.

15. Campbell, John P.; and Goodman, Alex: A Semiempirical Method for Estimating the Rolling Moment Due to Yawing of Airplanes. NACA TN 1984, 1949.

16. Anon.: Data Sheets – Aerodynamics. Vols. I, II, III, Roy. Aero. Soc.

17. Queijo, M. J.: Theoretical Span Load Distributions and Rolling Moments for Sideslipping Wings of Arbitrary Plan Form in Incompressible Flow. NACA Rep. 1269, 1956. (Supersedes NACA TN 3605.)

18. DeYoung, John; and Harper, Charles W.: Theoretical Symmetric Span Loading at Subsonic Speeds for Wings Having Arbitrary Plan Form. NACA Rep. 921, 1948.

19. Campbell, George S.: A Finite-Step Method for the Calculation of Span Loadings of Unusual Plan Forms. NACA RM L50L13, 1951.

20. Gray, W. L.; and Schenk, K. M.: A Method for Calculating the Subsonic Steady-State Loading on an Airplane With a Wing of Arbitrary Plan Form and Stiffness. NACA TN 3030, 1953.

21. Diederich, Franklin W.; and Zlotnick, Martin: Calculated Spanwise Lift Distributions, Influence Functions, and Influence Coefficients for Unswept Wings in Subsonic Flow. NACA Rep. 1228, 1955. (Supersedes NACA TN 3014.)

22. Diederich, Franklin W.; and Latham, W. Owen: Calculated Aerodynamic Loadings of M, W, and Λ Wings in Incompressible Flow. NACA RM L51E29, 1951.

23. Jacobs, W.: Systematische Druckverteilungsmessungen an Pfeilflügeln konstanter Tiefe bei symmetrischer und unsymmetrischer Anströmung. Bericht 44/28, Aerodynamisches Institut der T. H. Braunschweig, Nov. 8, 1944.

24. Fisher, Lewis R.: Approximate Corrections for the Effects of Compressibility on the Subsonic Stability Derivatives of Swept Wings. NACA TN 1854, 1949.

25. Bird, J. D.: Some Theoretical Low-Speed Span Loading Characteristics of Swept Wings in Roll and Sideslip. NACA Rep. 969, 1950. (Supersedes NACA TN 1839.)

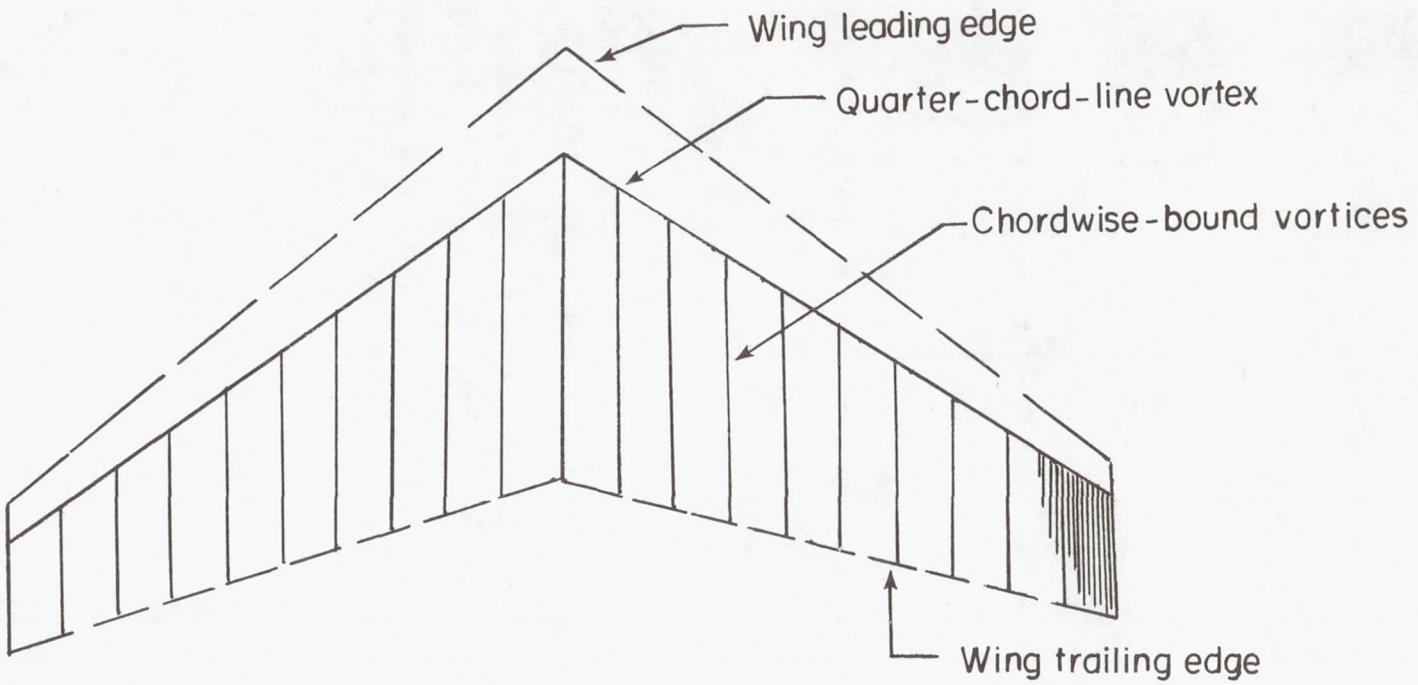

Figure 1.- Bound-vortex system used to represent a wing in all types of flow.

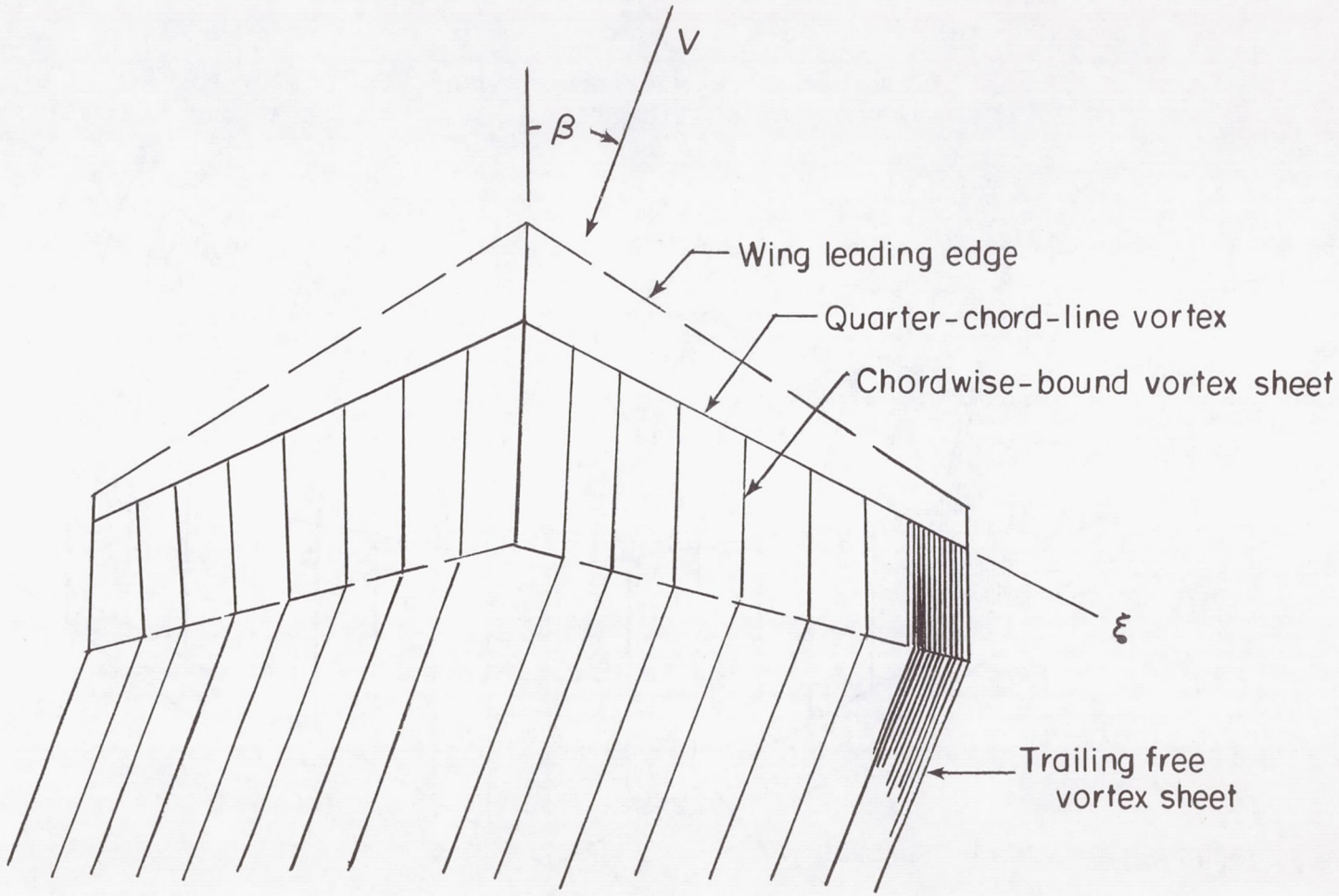

Figure 2.- Complete vortex system for a wing in sideslip.

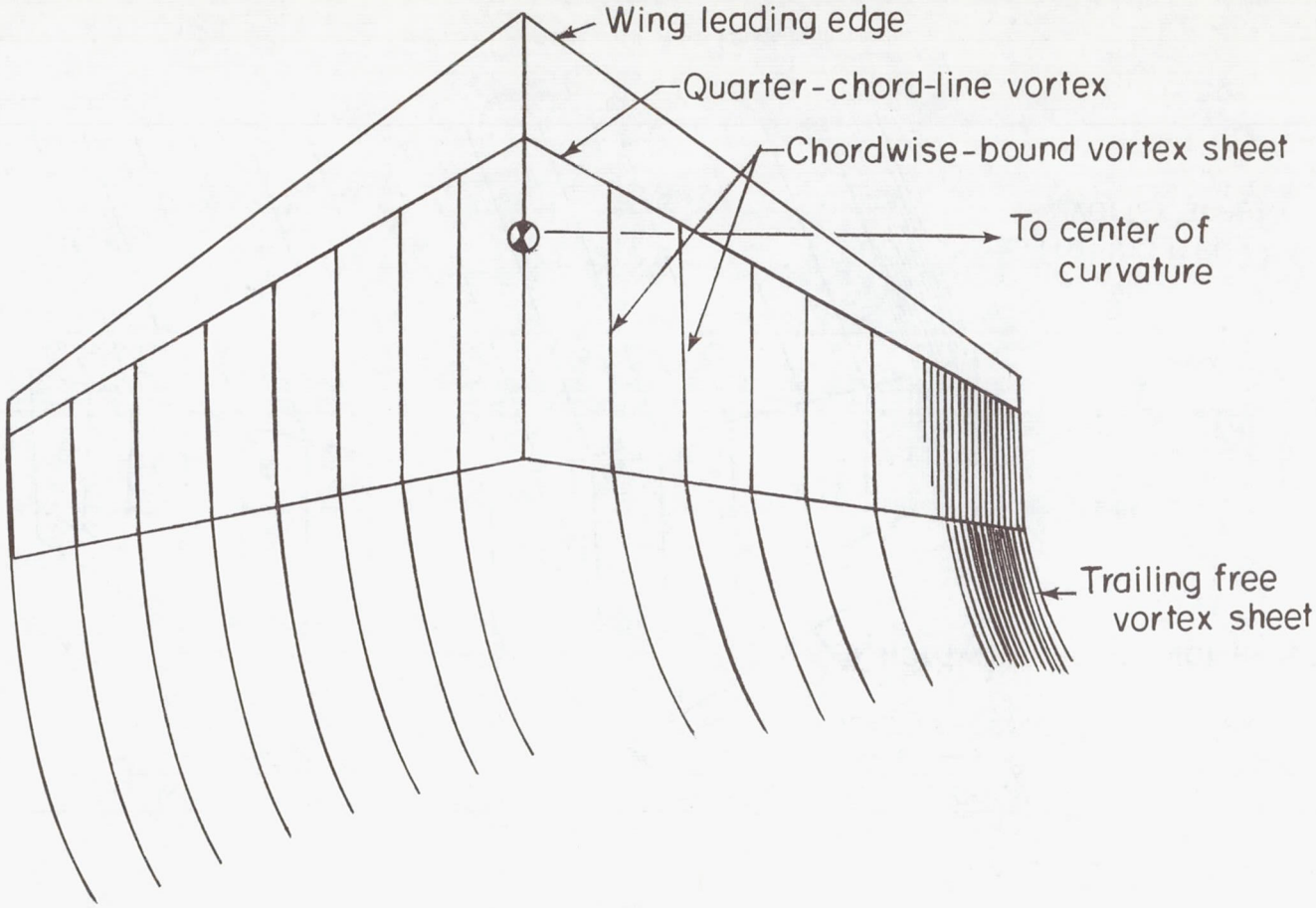

Figure 3.- Complete vortex system for the yawing wing.

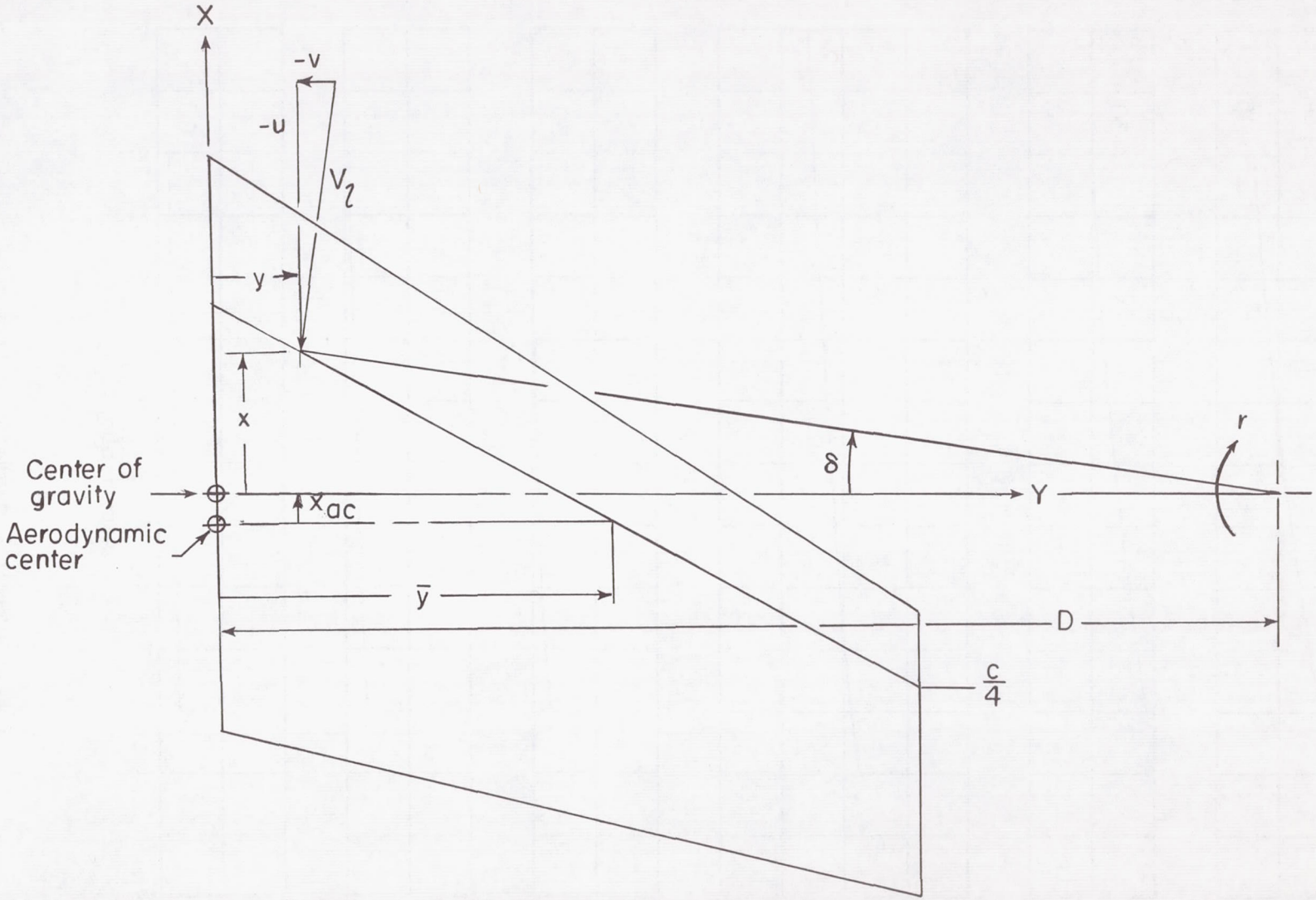

Figure 4.- Details of wing geometry and wind velocity components for yawing wing.

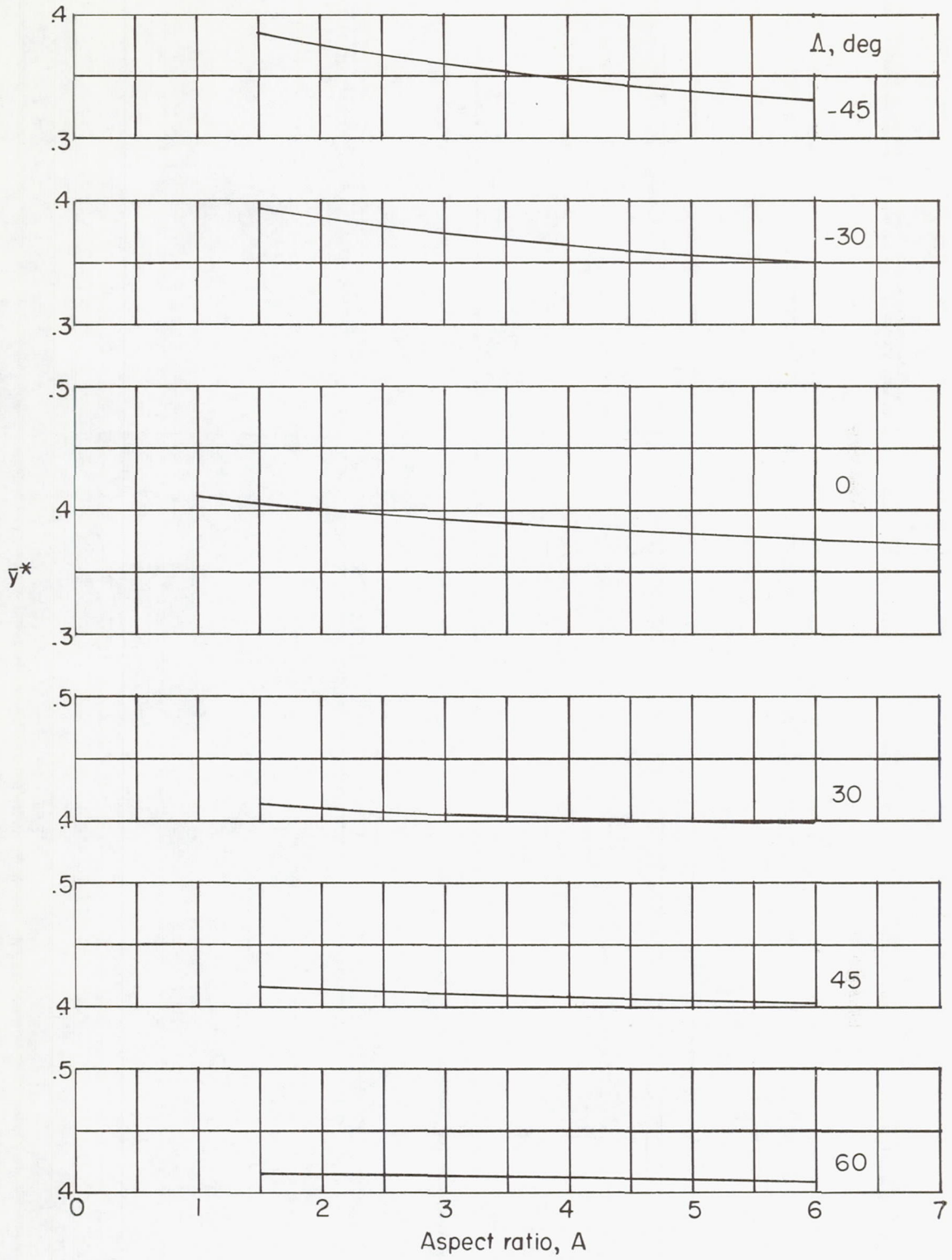

(a) $\lambda = 0$.

Figure 5.- Spanwise location of centroid of angle-of-attack loading.

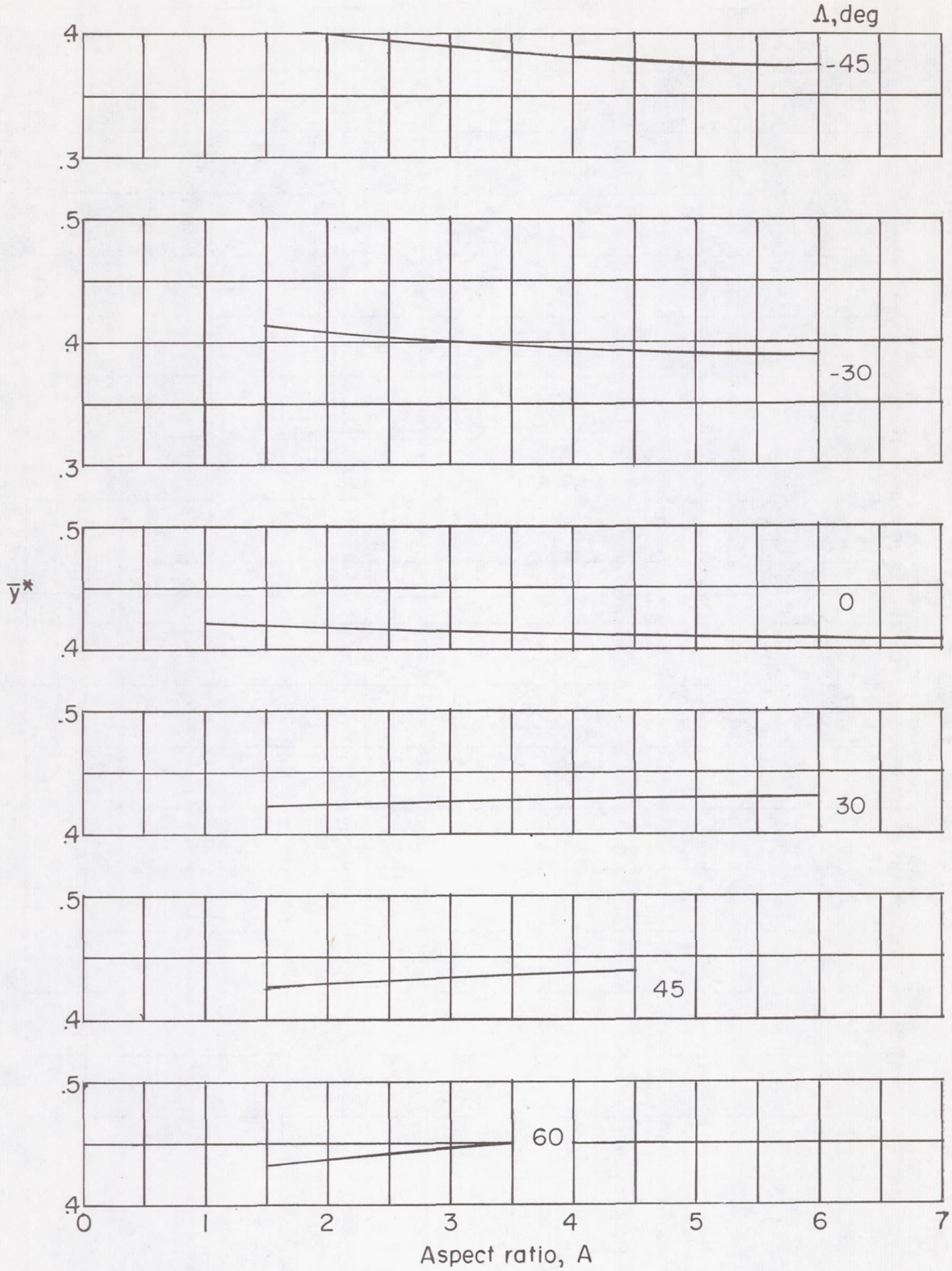

(b) $\lambda = 0.25$.

Figure 5.- Continued.

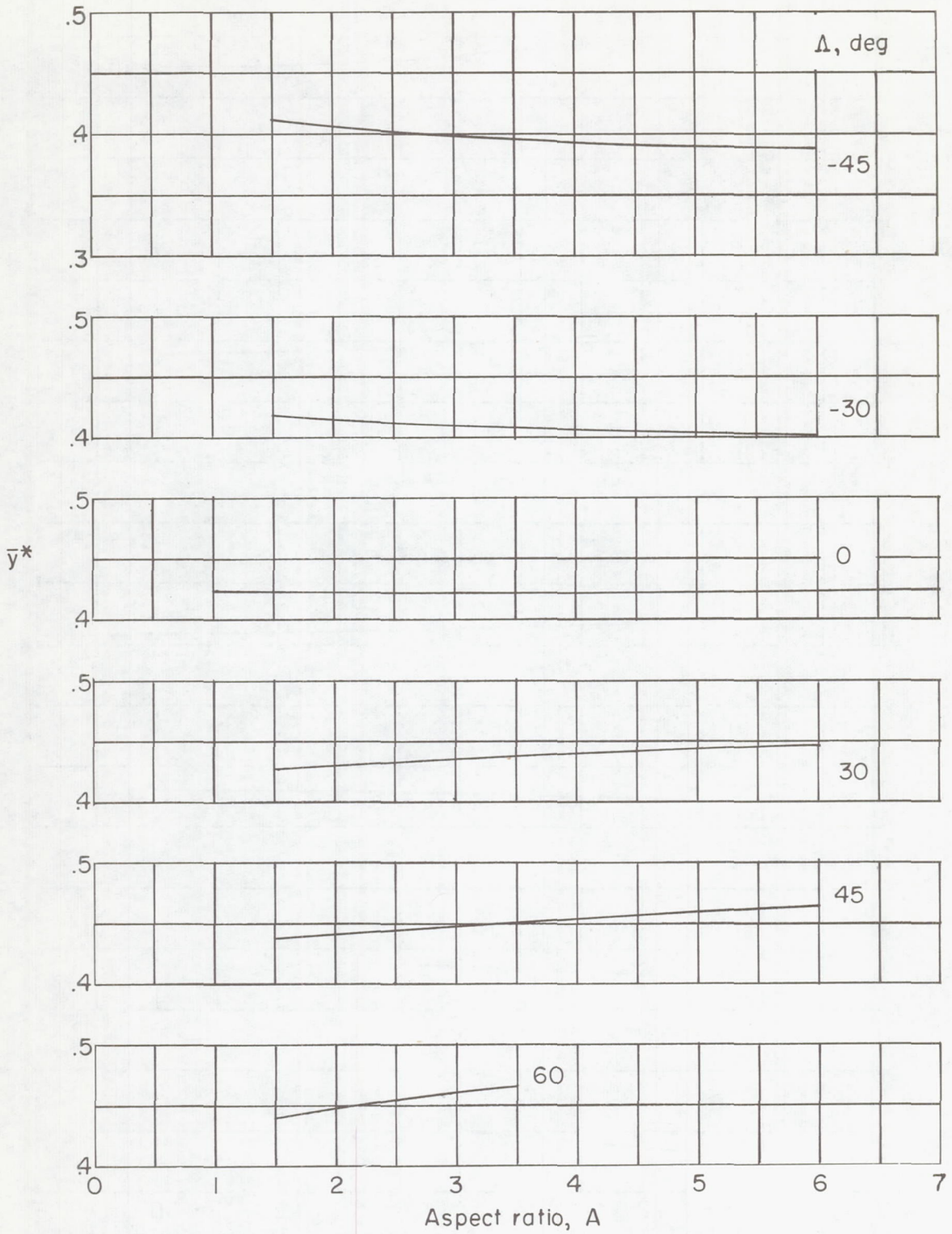

(c) $\lambda = 0.5$.

Figure 5.- Continued.

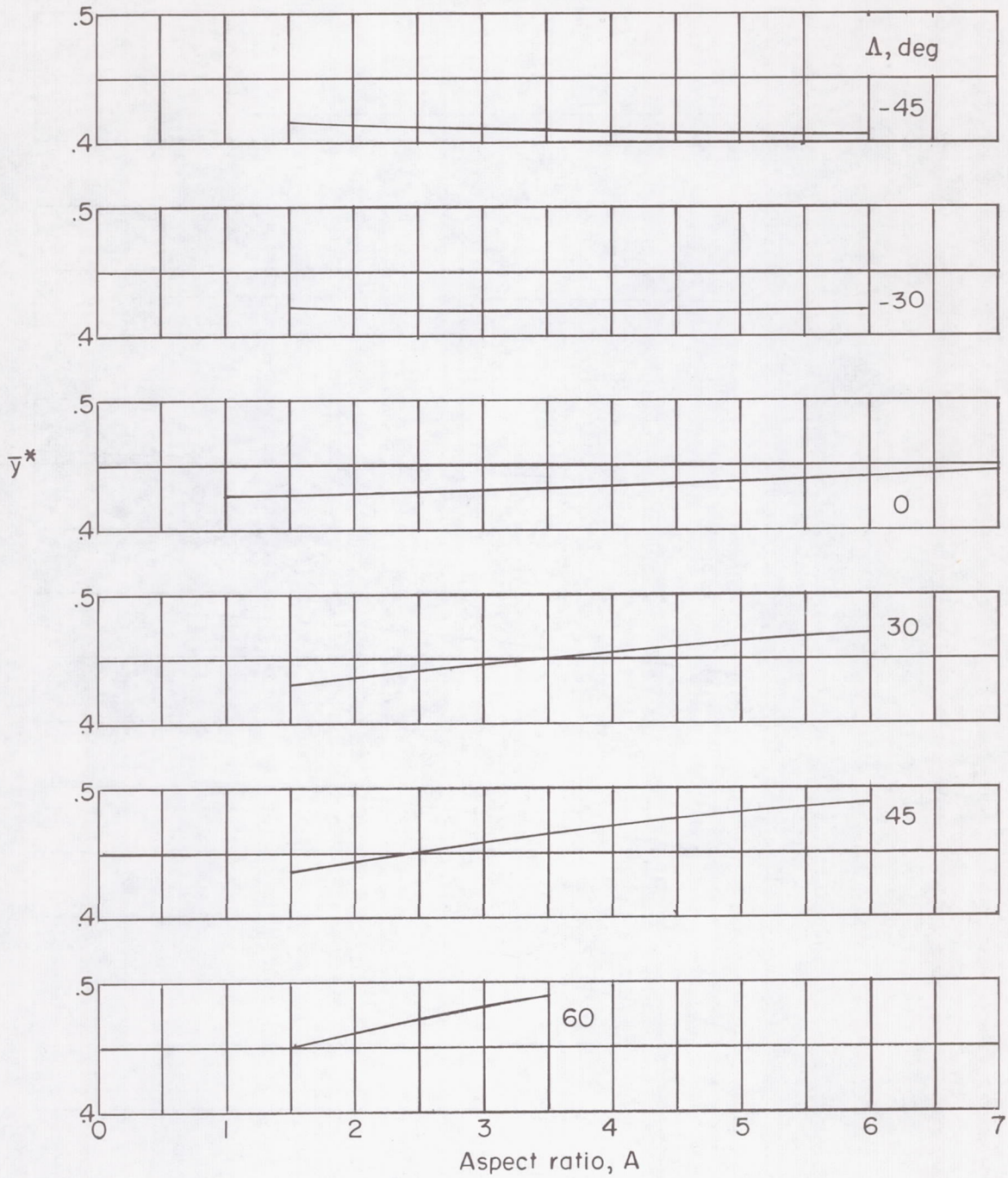

(d) $\lambda = 1.0$.

Figure 5.- Continued.

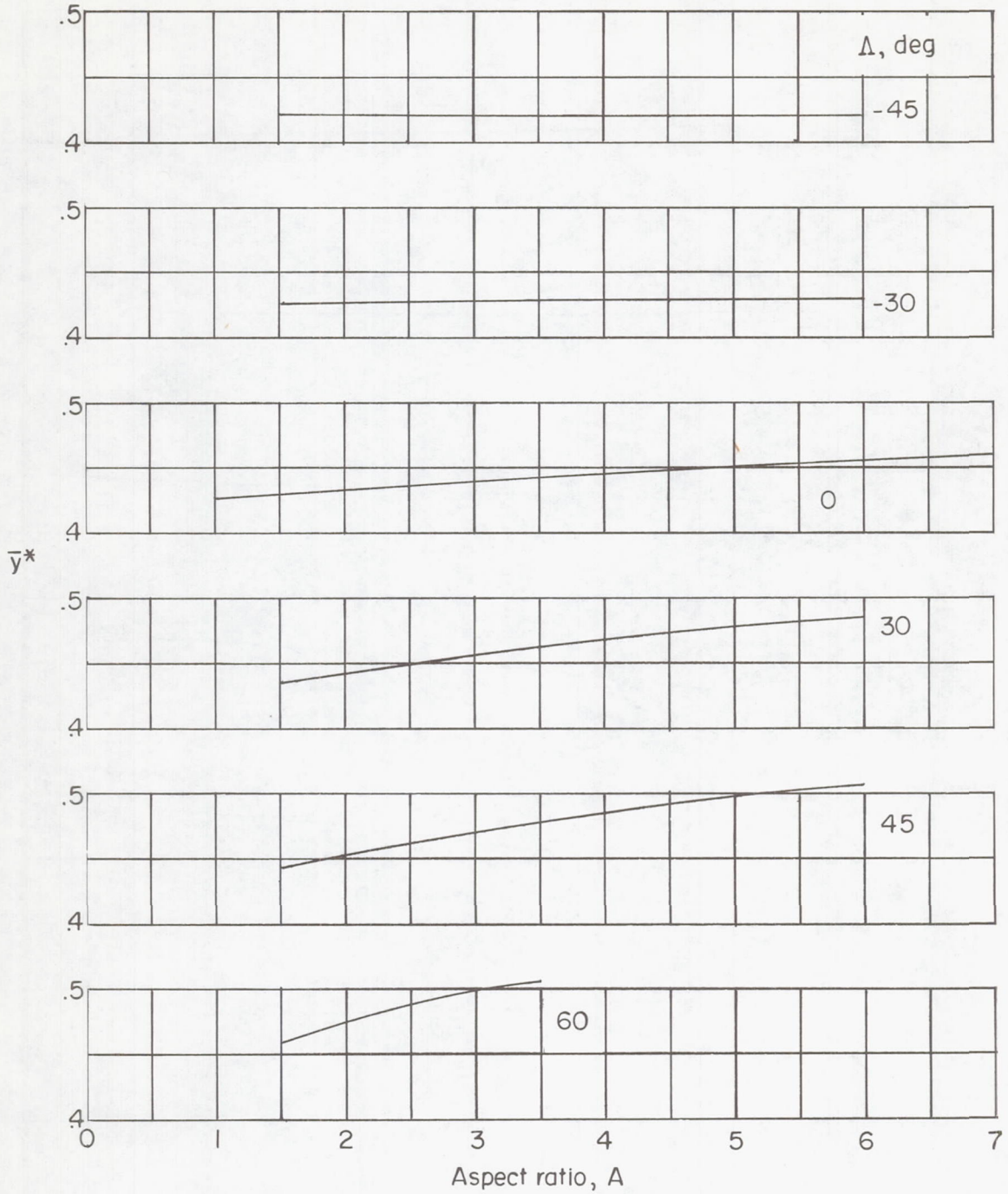

(e) $\lambda = 1.5$.

Figure 5.- Concluded.

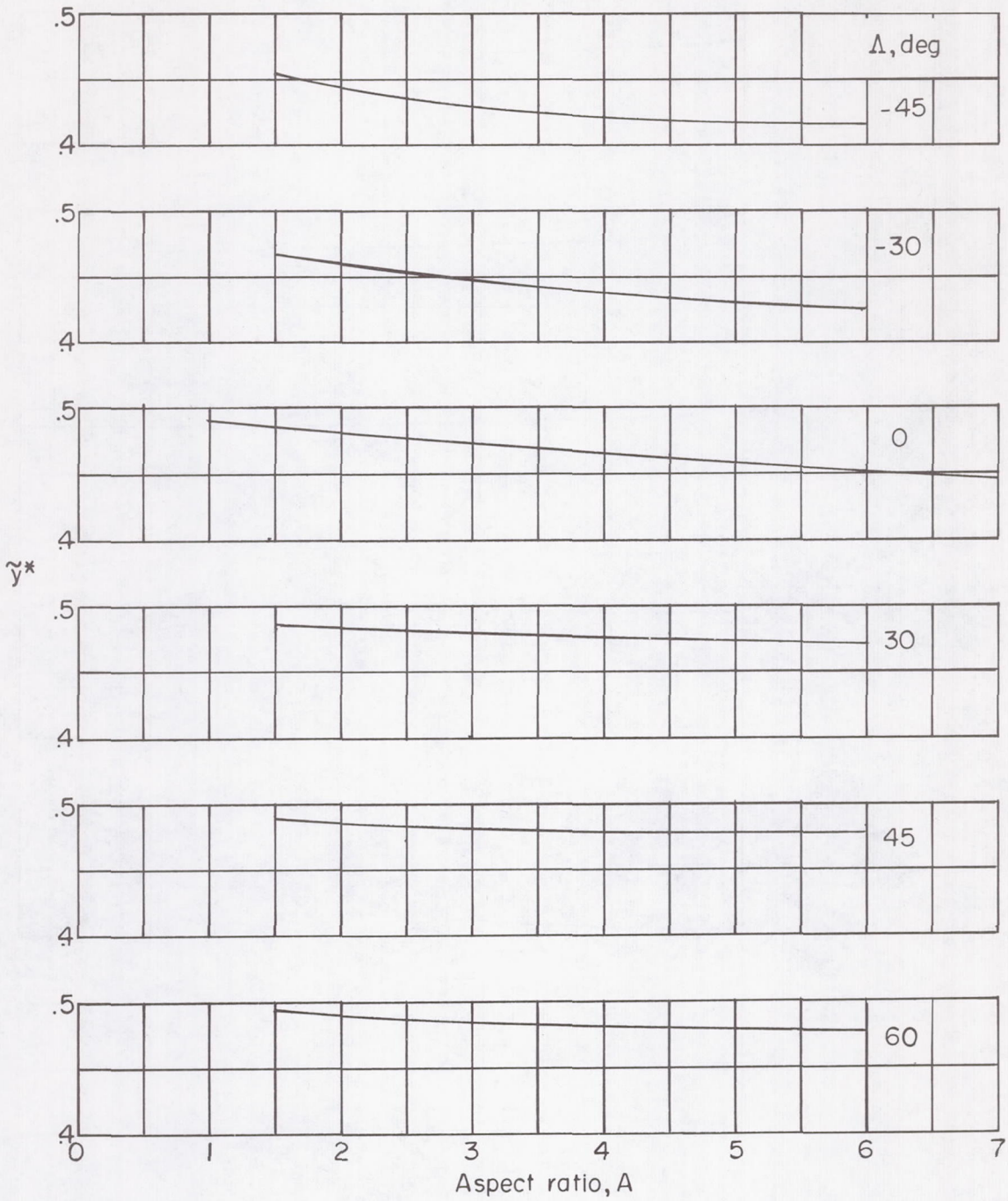

(a) $\lambda = 0$.

Figure 6.- Spanwise location of radius of gyration for angle-of-attack span load.

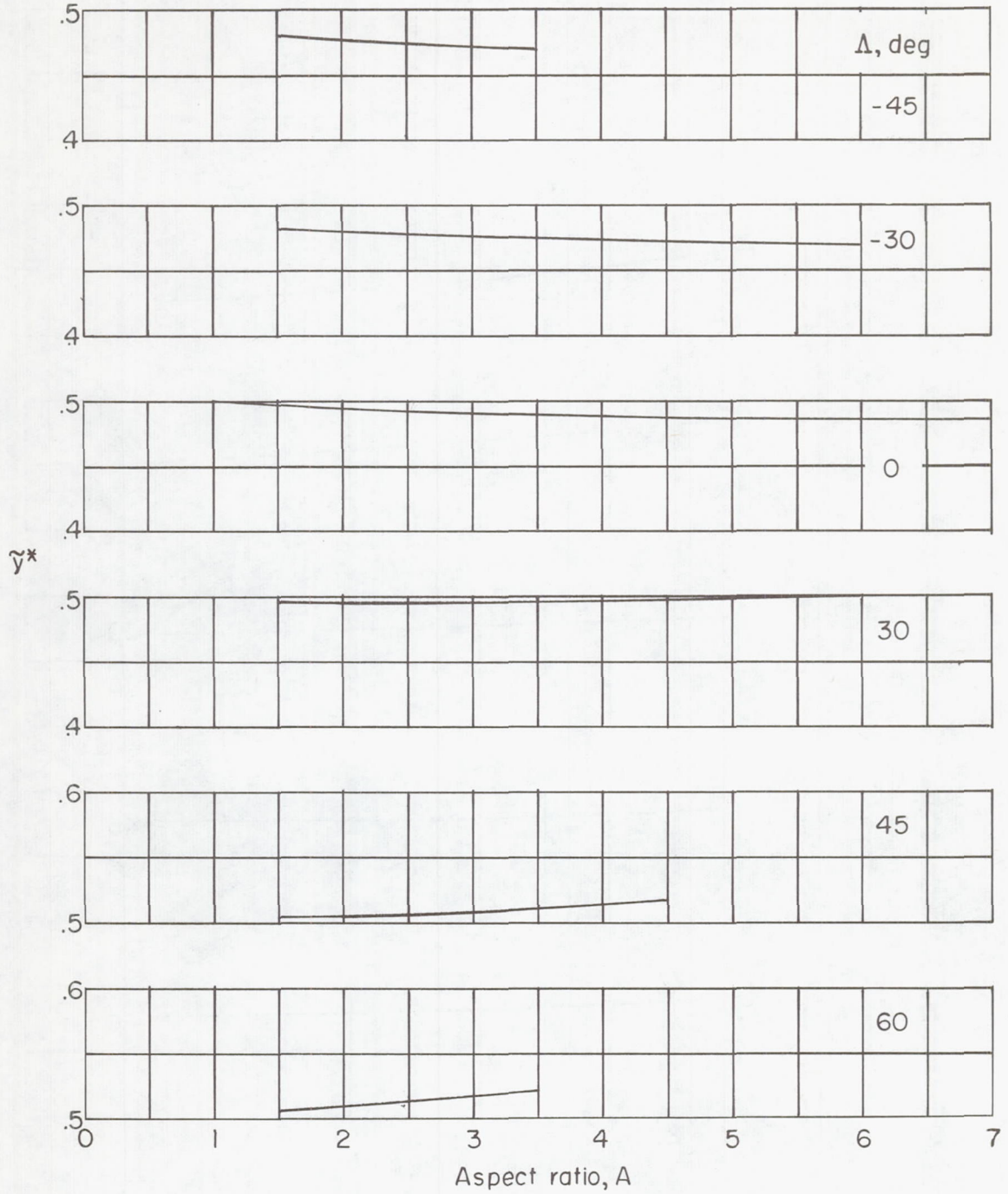

(b) $\lambda = 0.25$.

Figure 6.- Continued.

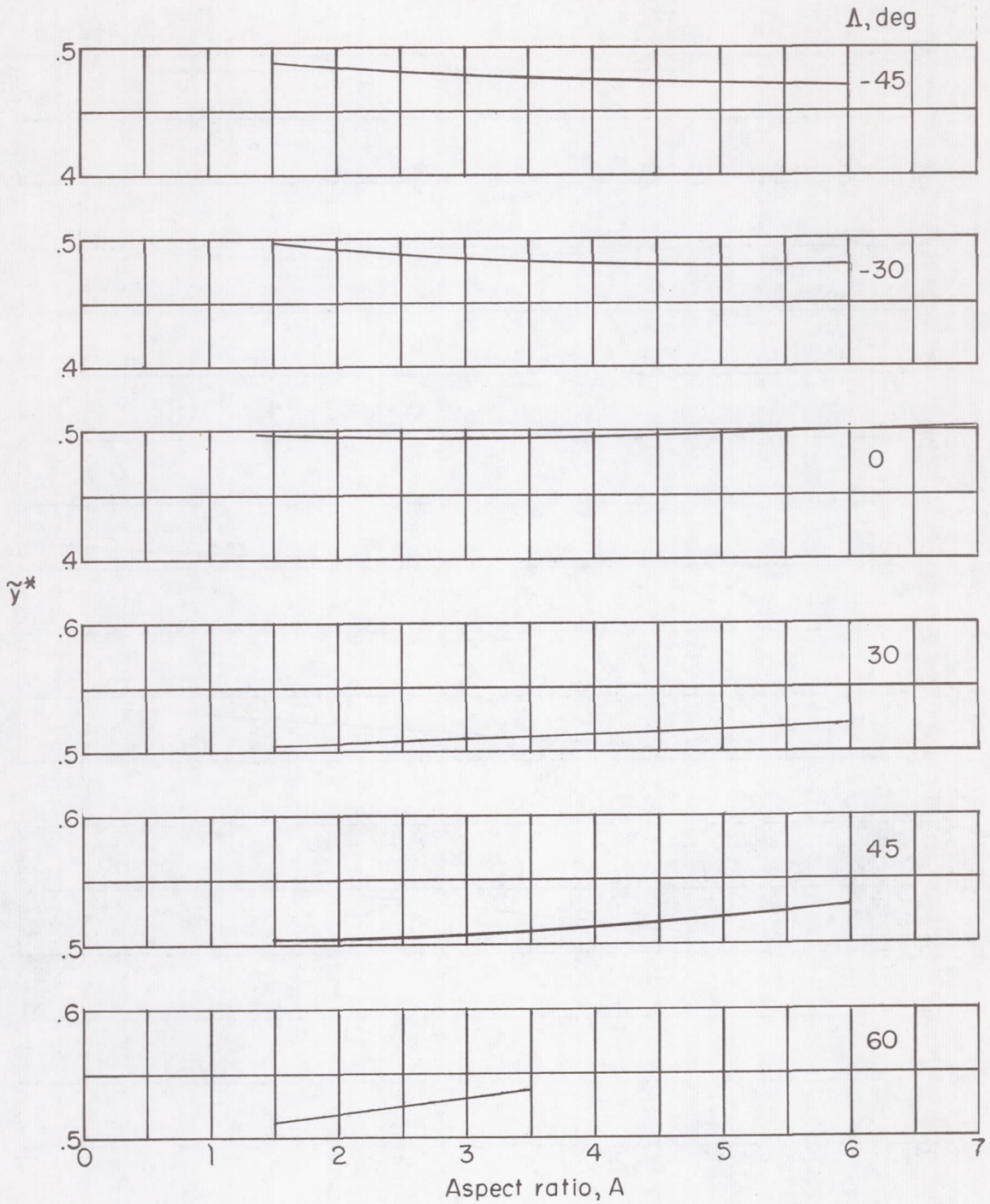

(c) $\lambda = 0.5$.

Figure 6.- Continued.

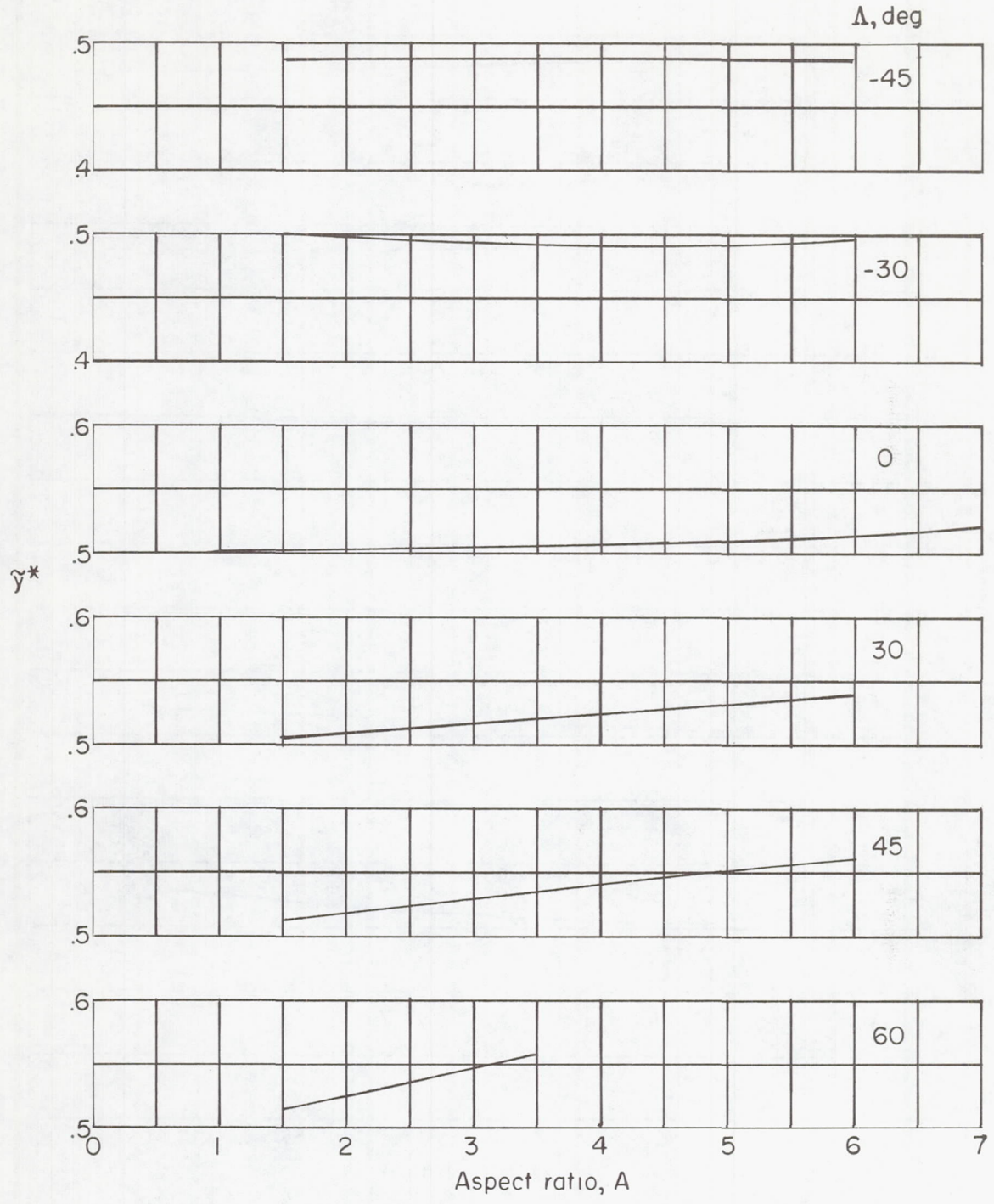

(d) $\lambda = 1.0$.

Figure 6.- Continued.

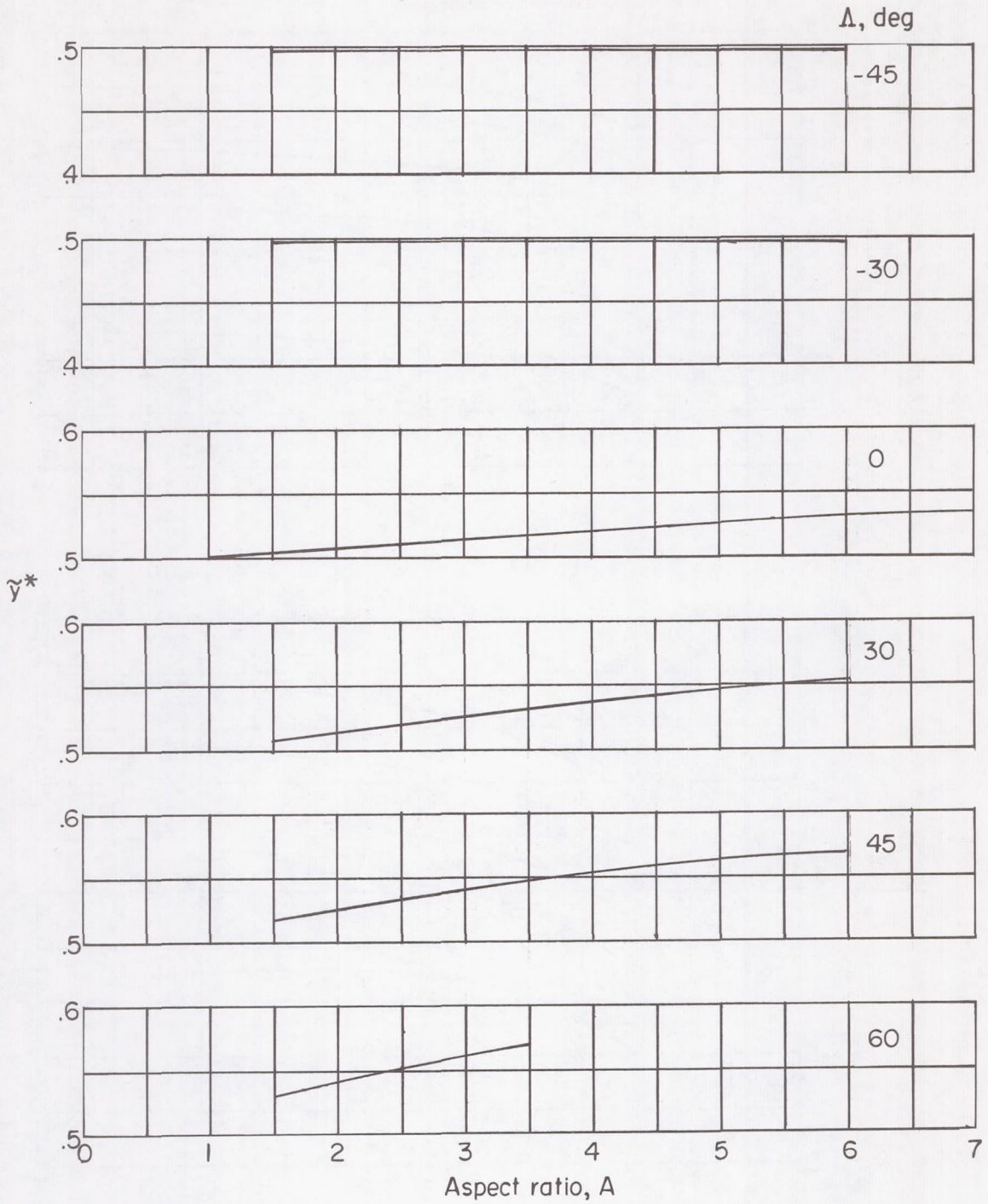

(e) $\lambda = 1.5$.

Figure 6.- Concluded.

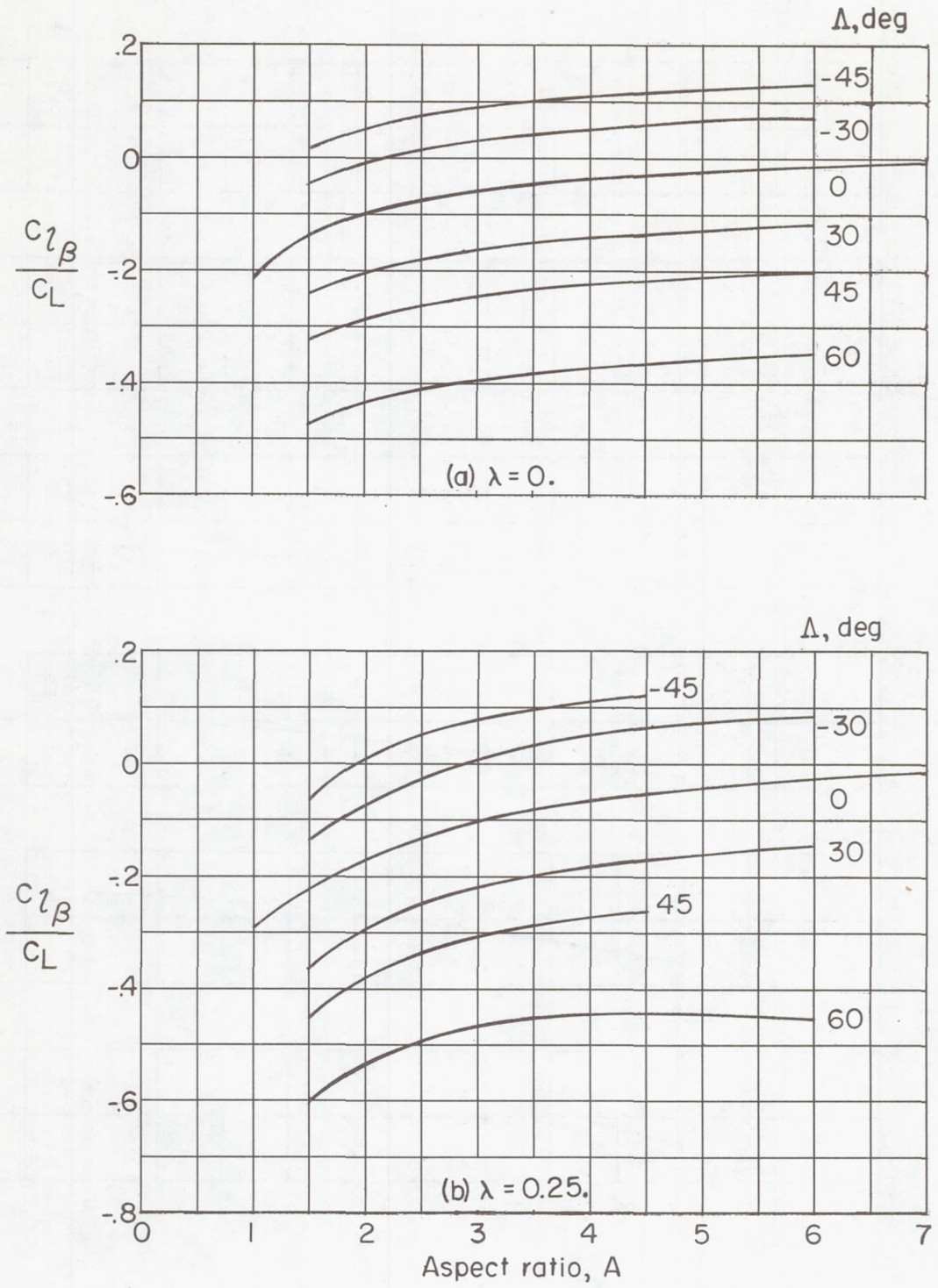

Figure 7.- Variation of C_{l_β}/C_L with aspect ratio, sweep, and taper ratio. M = 0; $x^*_{ac} = 0$.

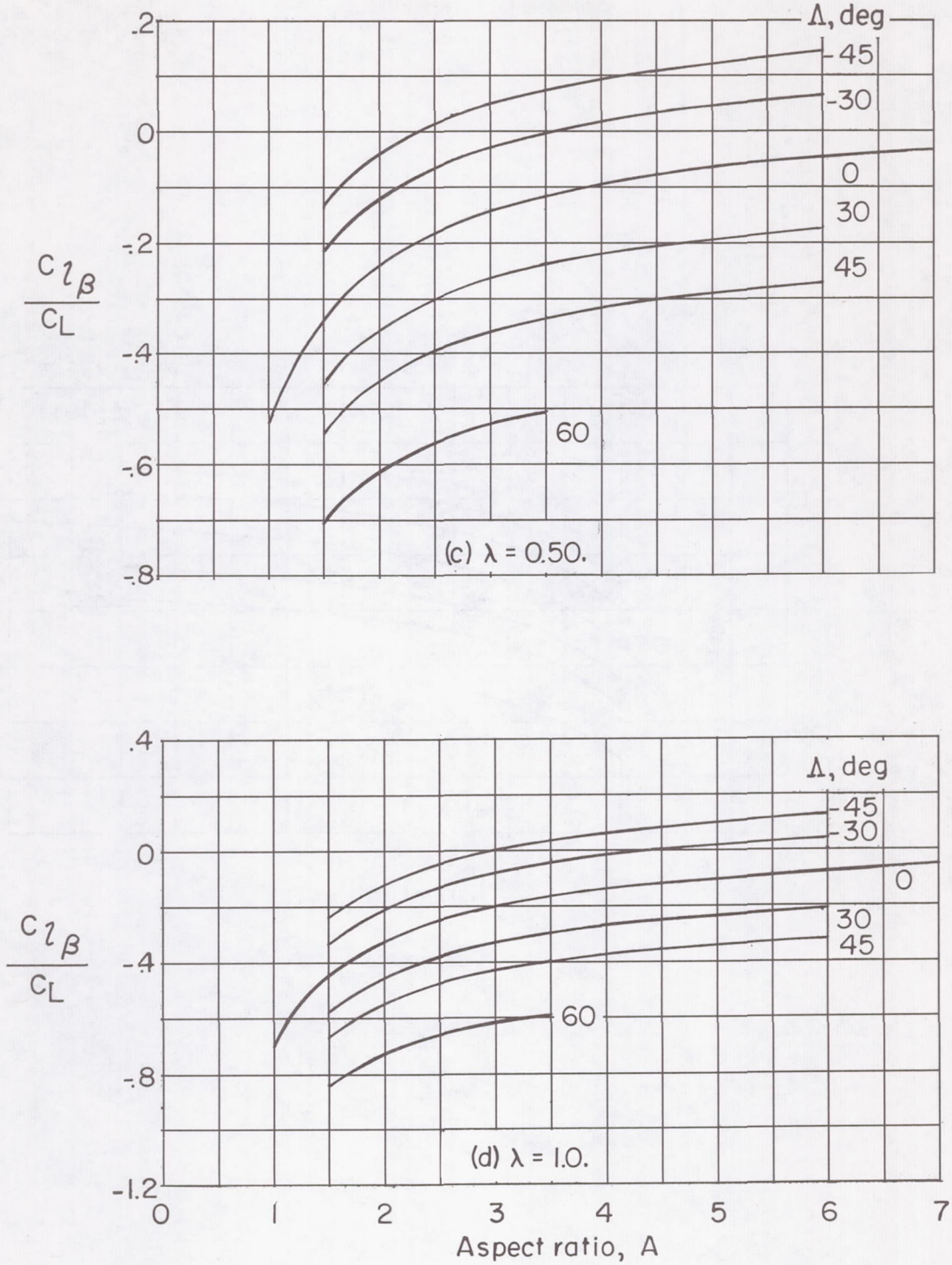

Figure 7.- Continued.

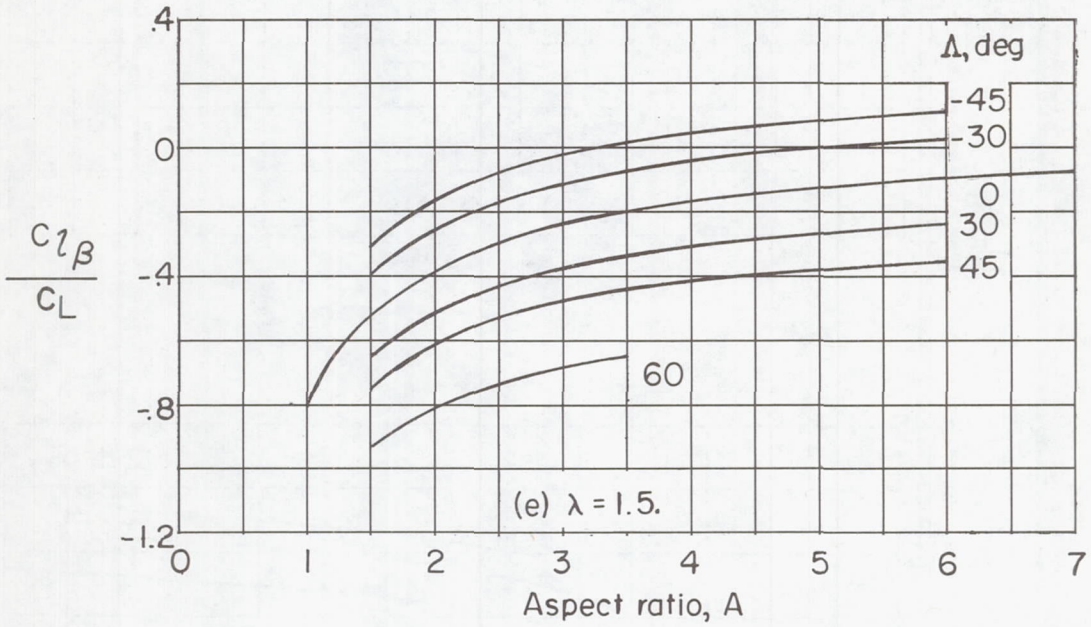

Figure 7.- Concluded.

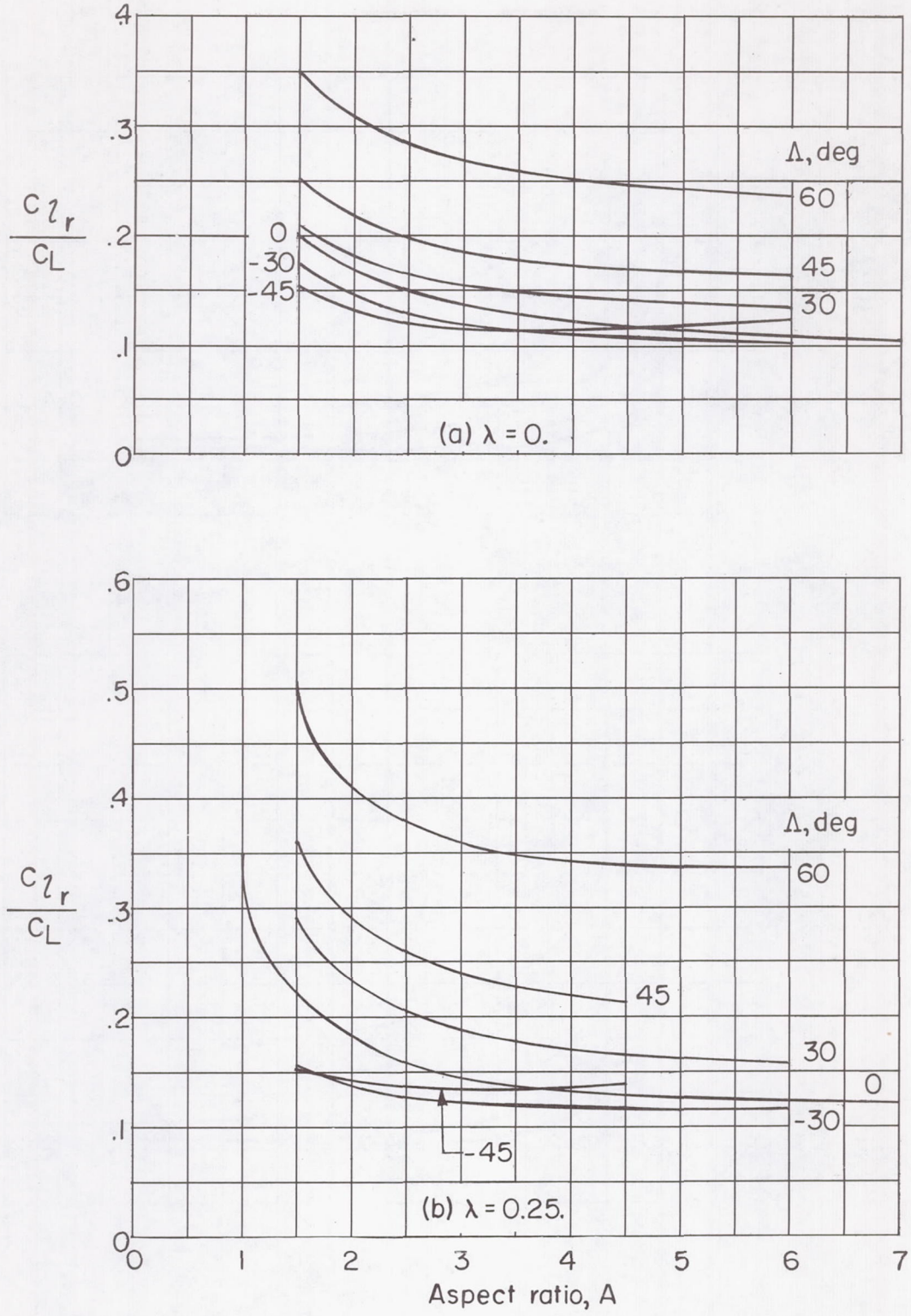

Figure 8.- Variation of C_{l_r}/C_L with aspect ratio, sweep, and taper ratio M = 0; x_{ac}^{*} = 0.

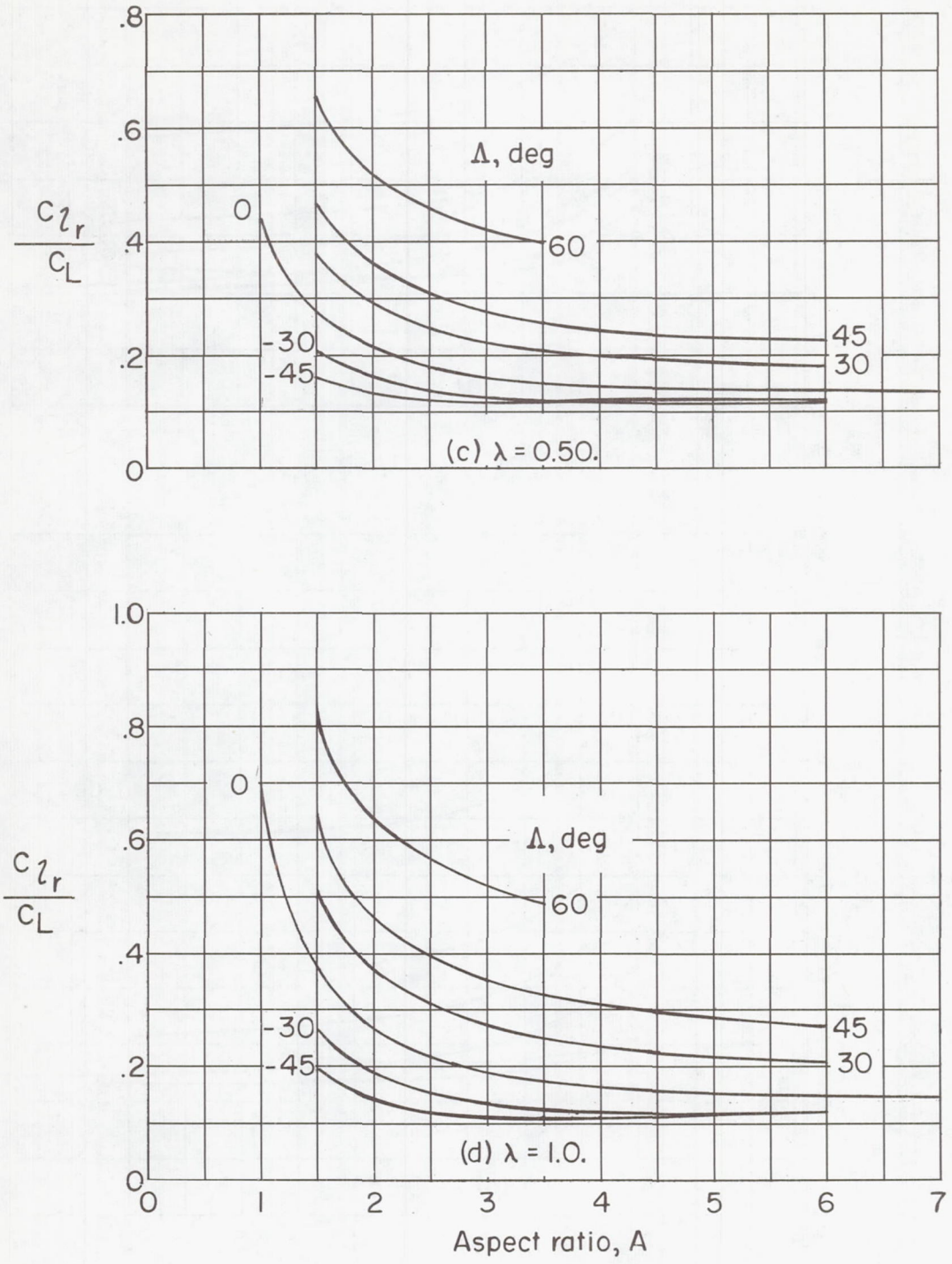

Figure 8.- Continued.

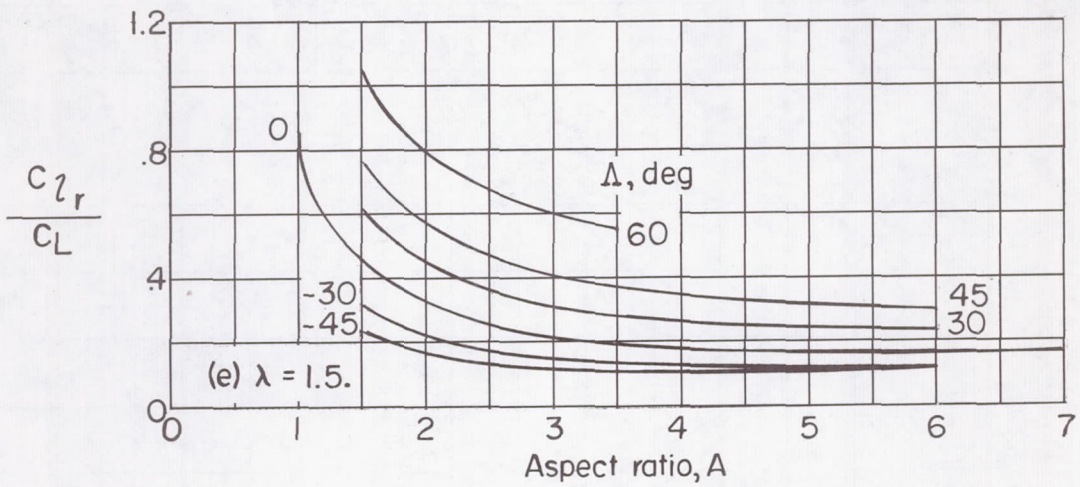

Figure 8.- Concluded.

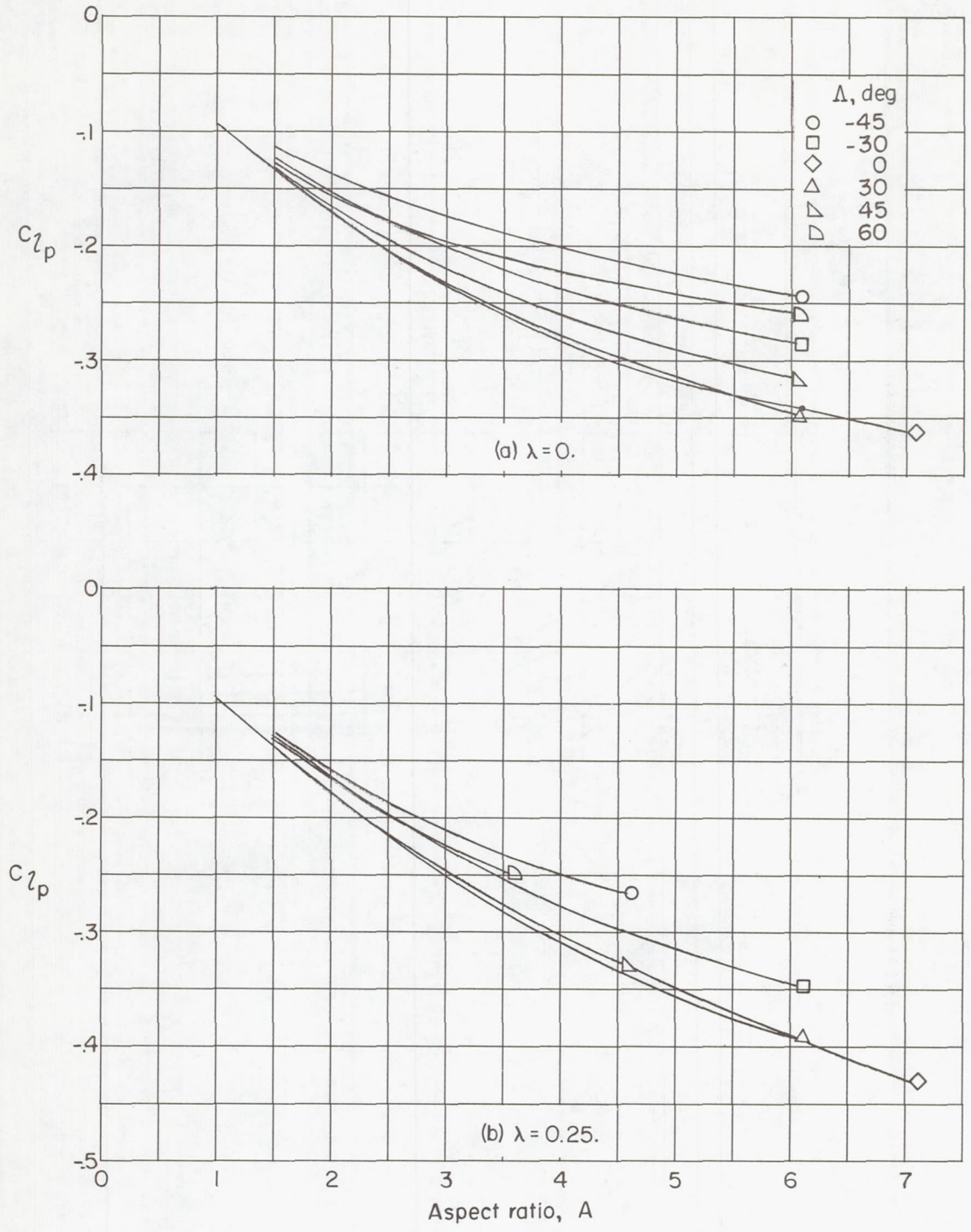

Figure 9.- Variation of C_{l_p} with aspect ratio, taper ratio, and sweep.

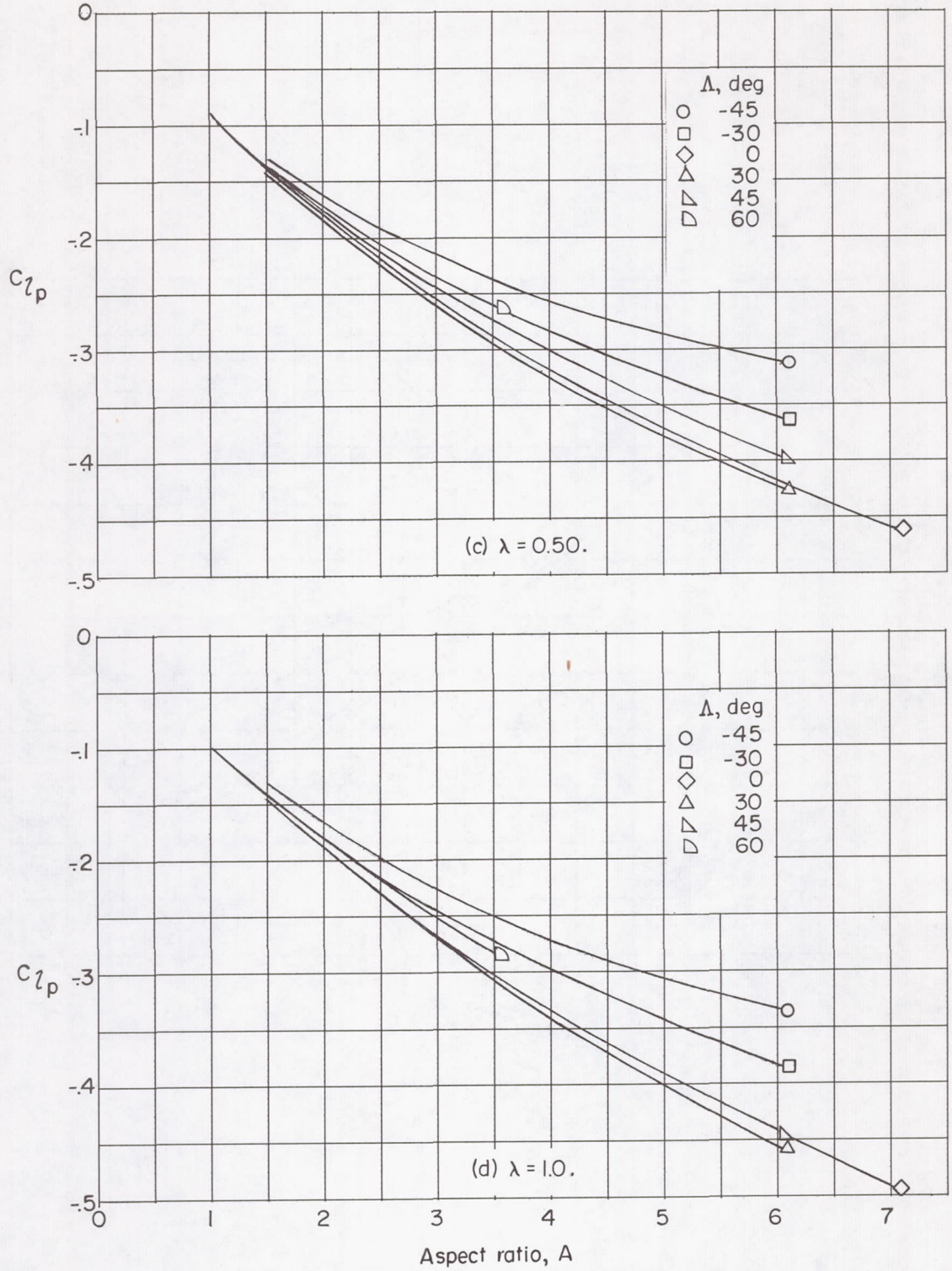

Figure 9.- Continued.

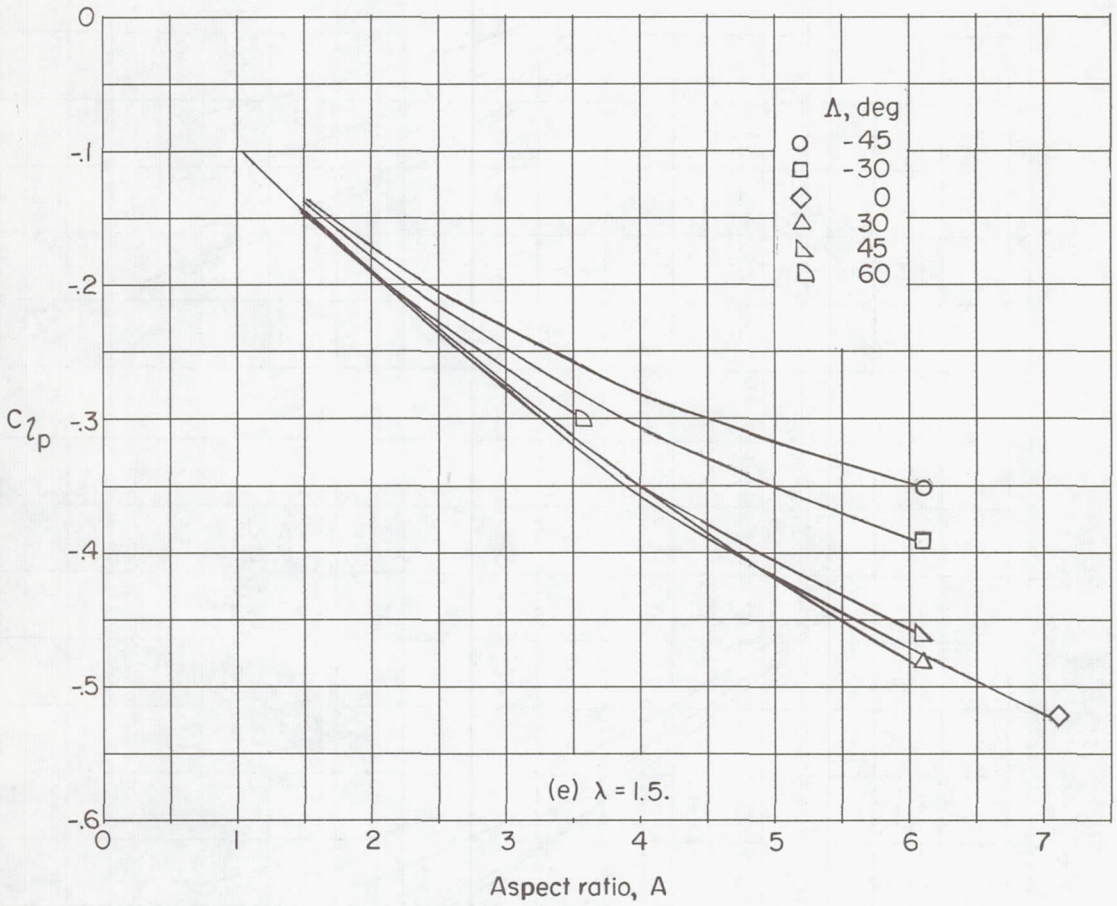

Figure 9.- Concluded.

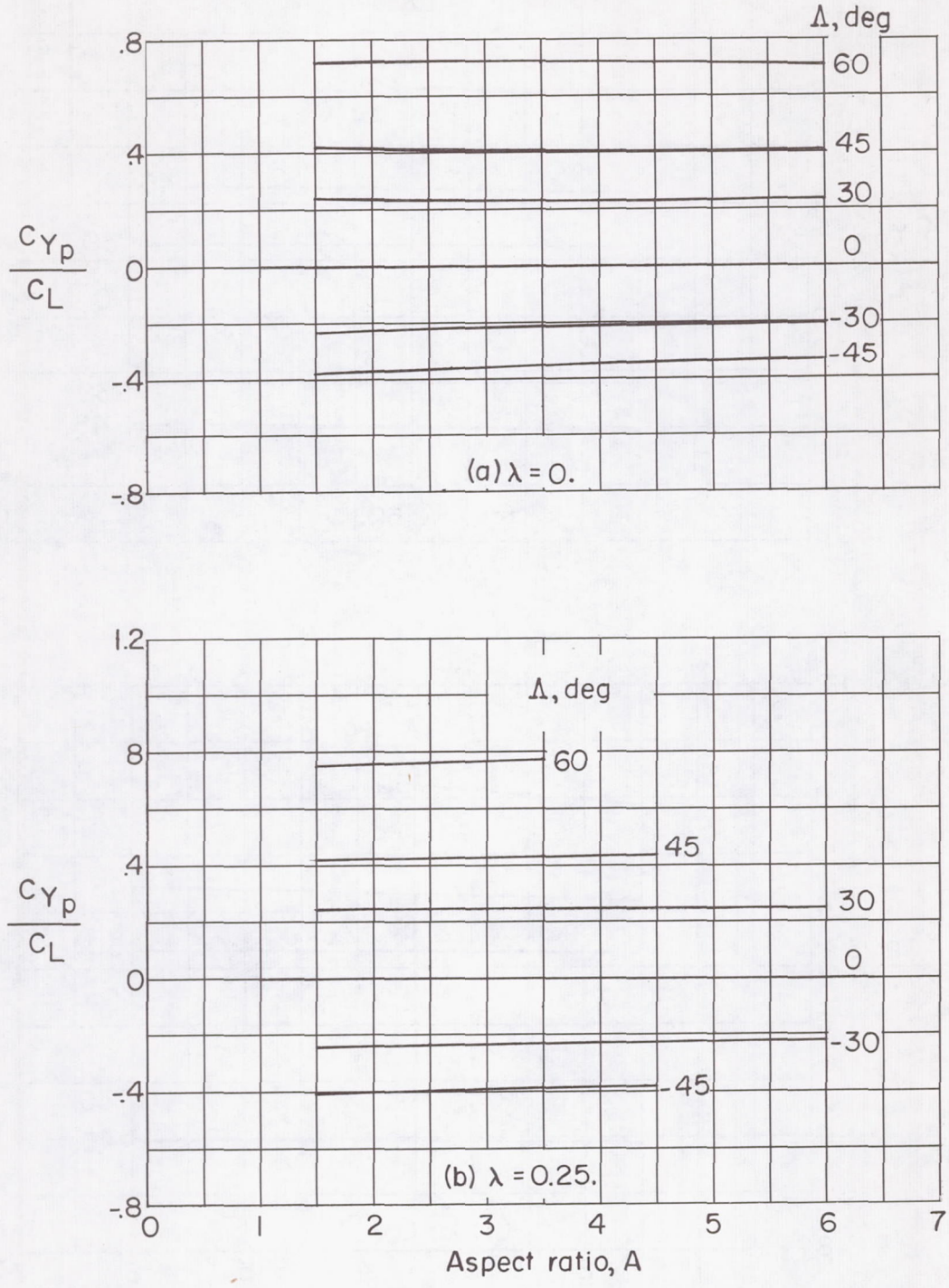

Figure 10.- Variation of C_{Y_p}/C_L with aspect ratio, sweep, and taper ratio. M = 0; $x_{ac}^{*} = 0$.

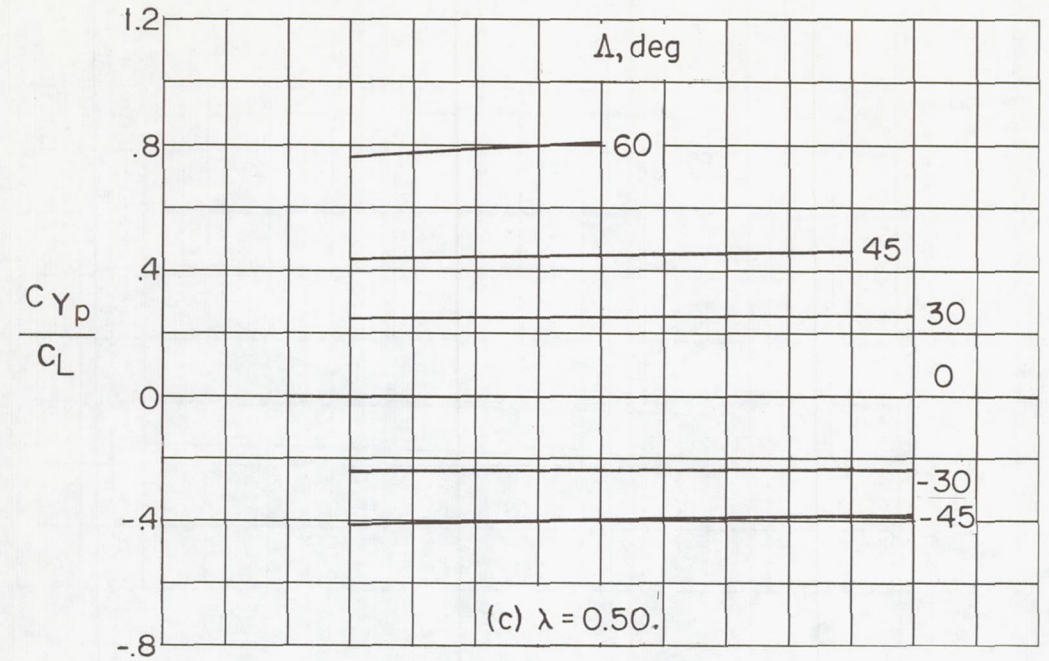

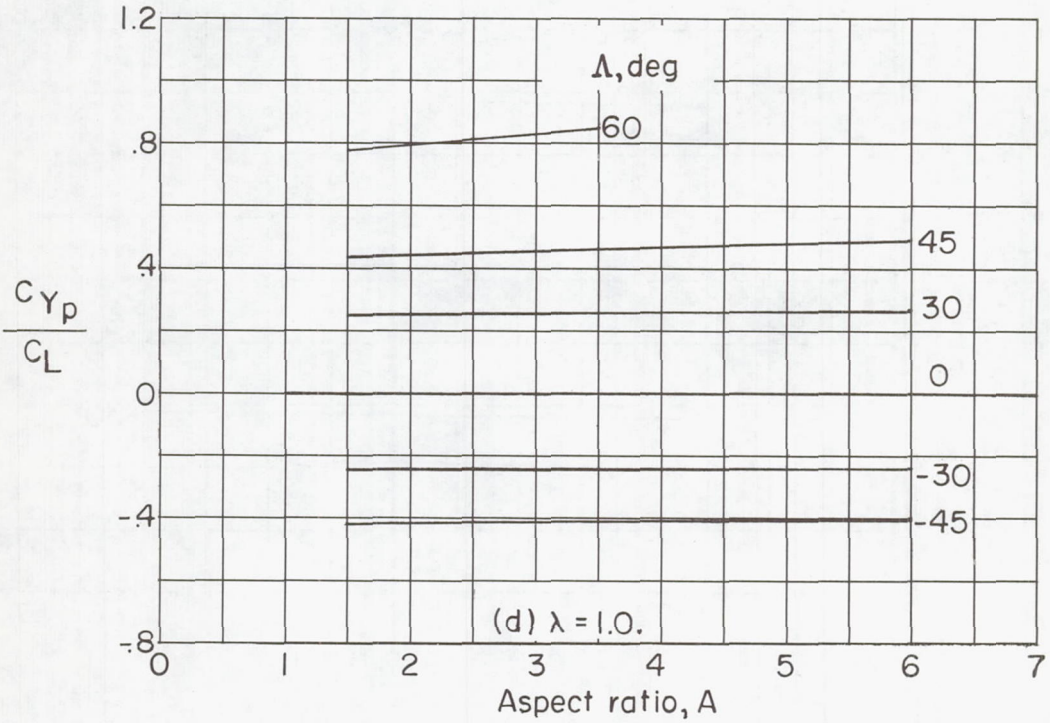

Figure 10.- Continued.

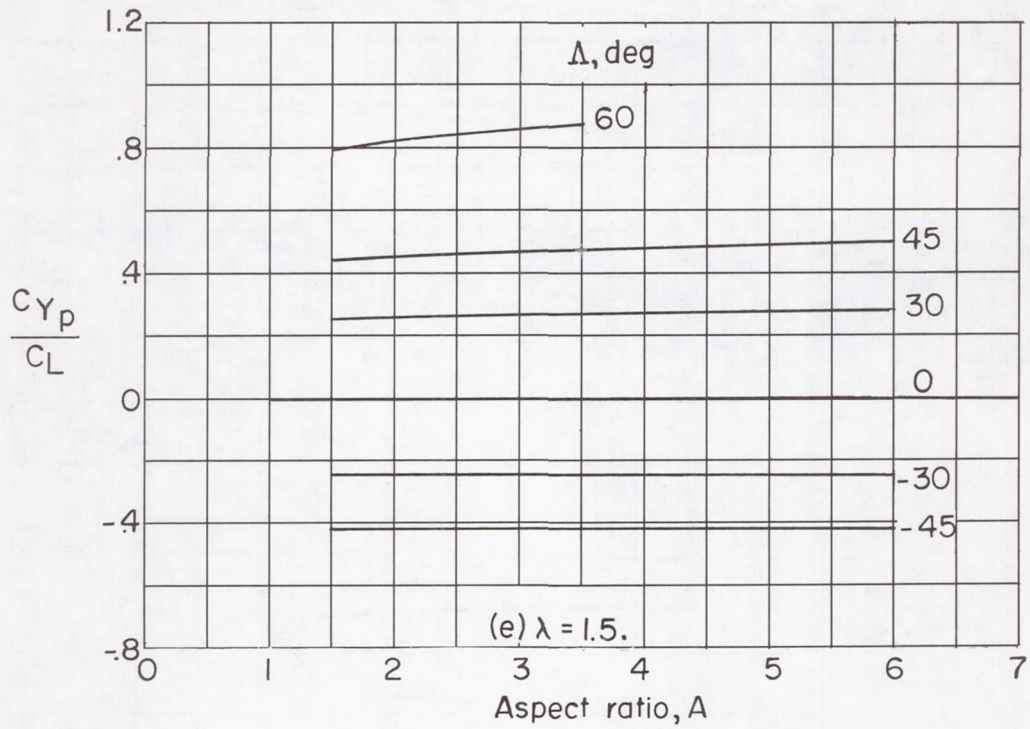

Figure 10.- Concluded.

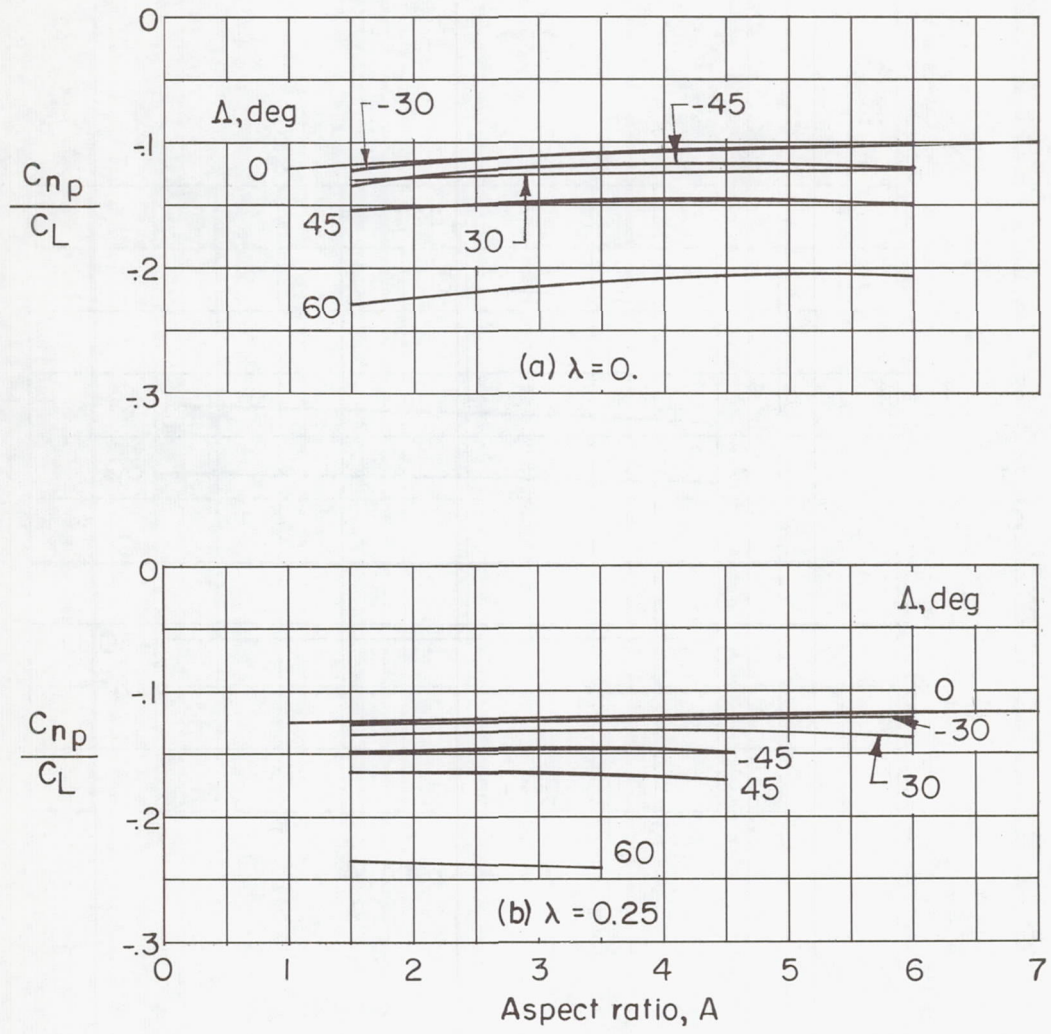

Figure 11.- Variation of C_{n_p}/C_L with aspect ratio, sweep, and taper ratio. M = 0; $x_{ac}^{*} = 0$.

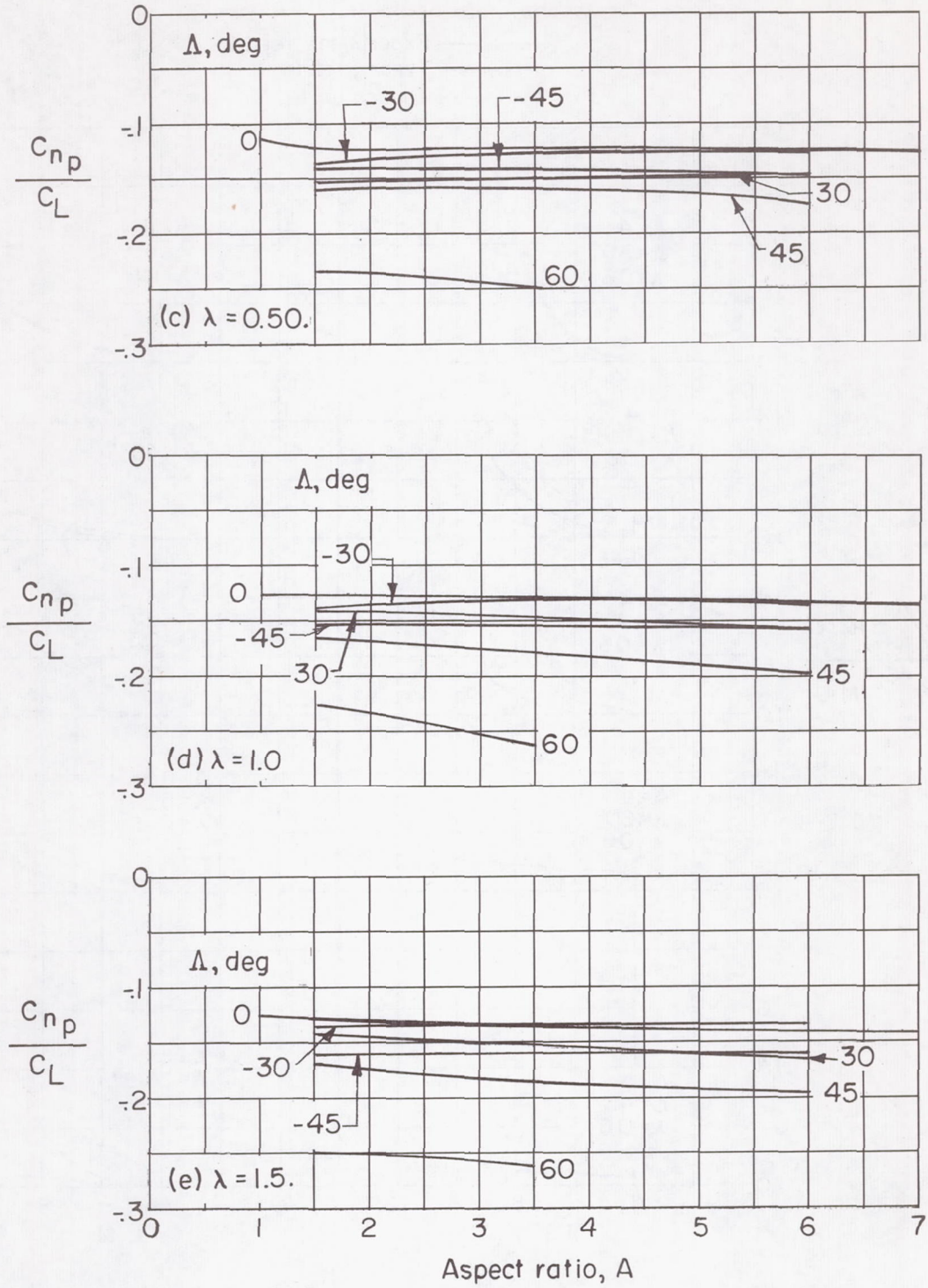

Figure 11.- Concluded.

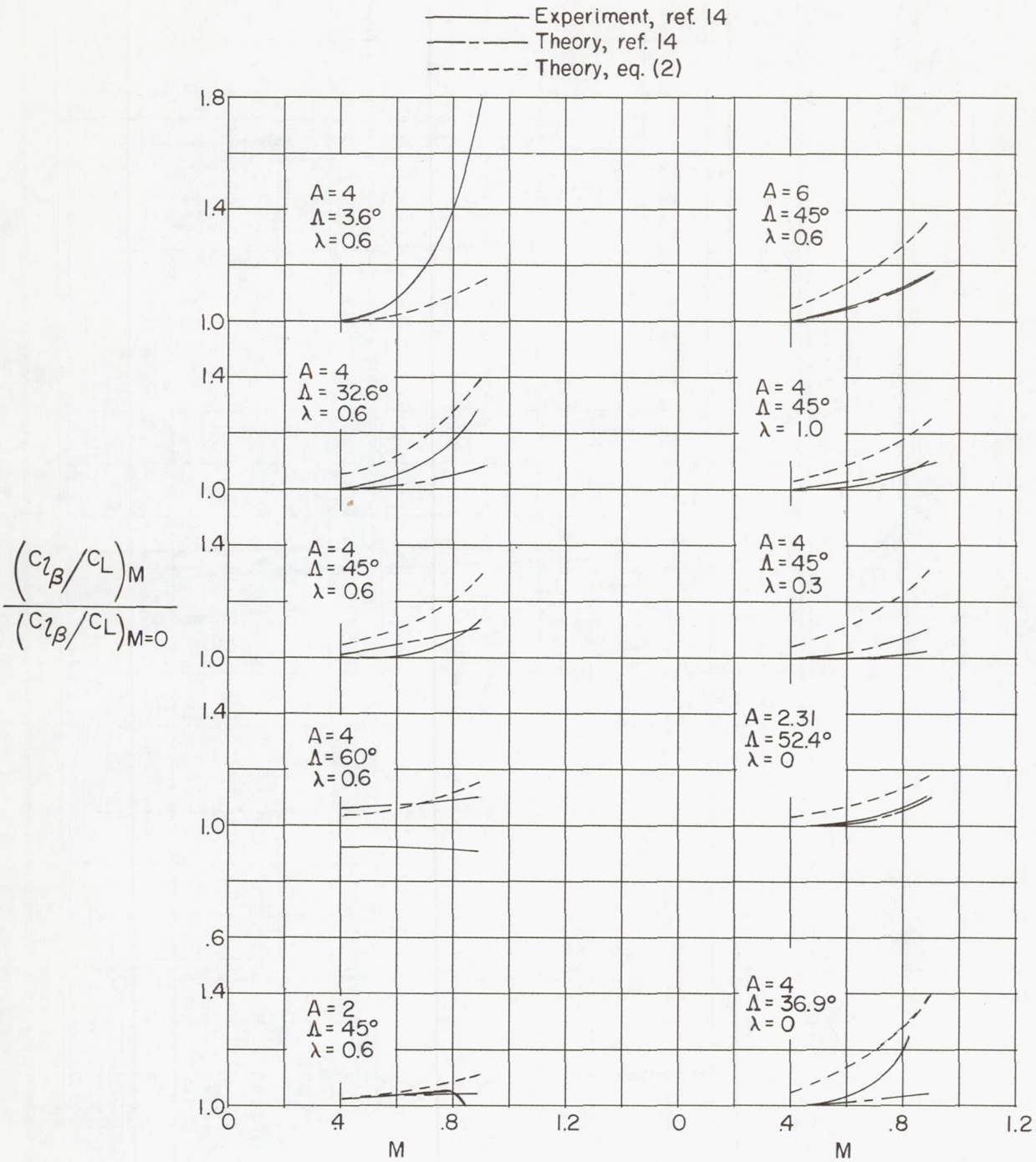

Figure 12.- Experimental and calculated effects of compressibility on C_{l_β}/C_L.

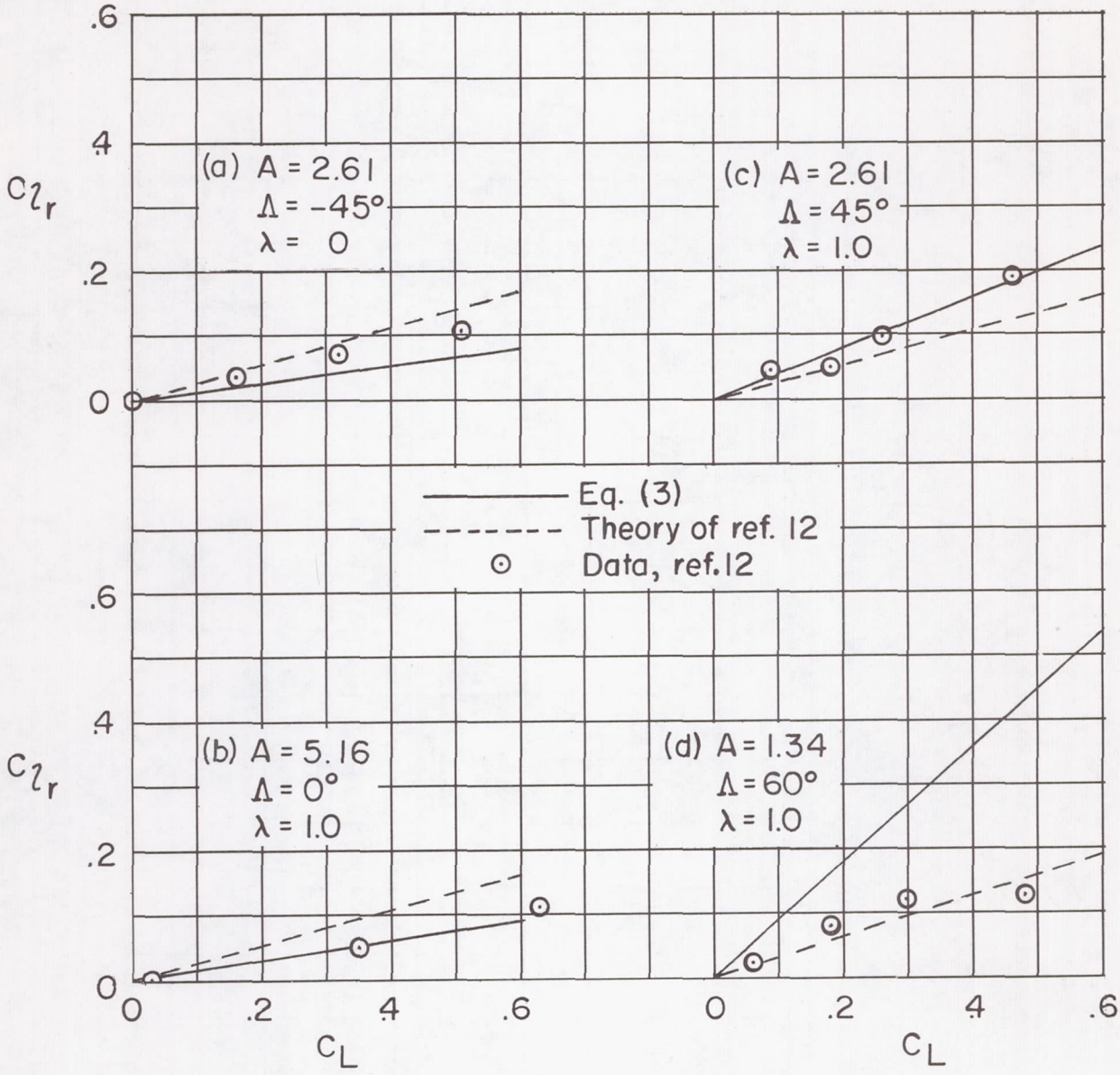

Figure 13.- Theoretical and experimental variations of C_{l_r} with C_L for several representative wings in incompressible flow.

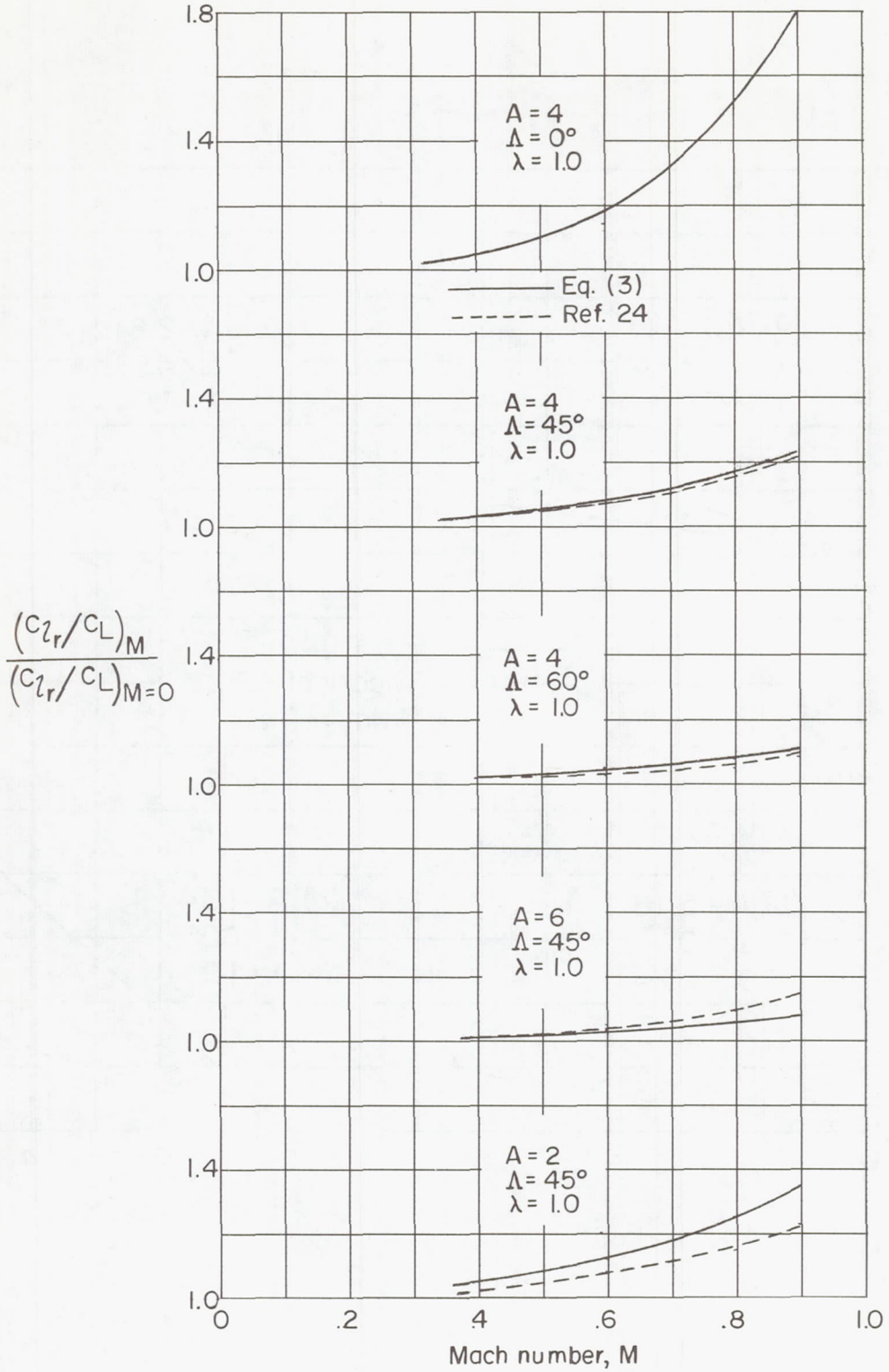

Figure 14.- Estimated effect of Mach number on the parameter C_{l_r}/C_L.

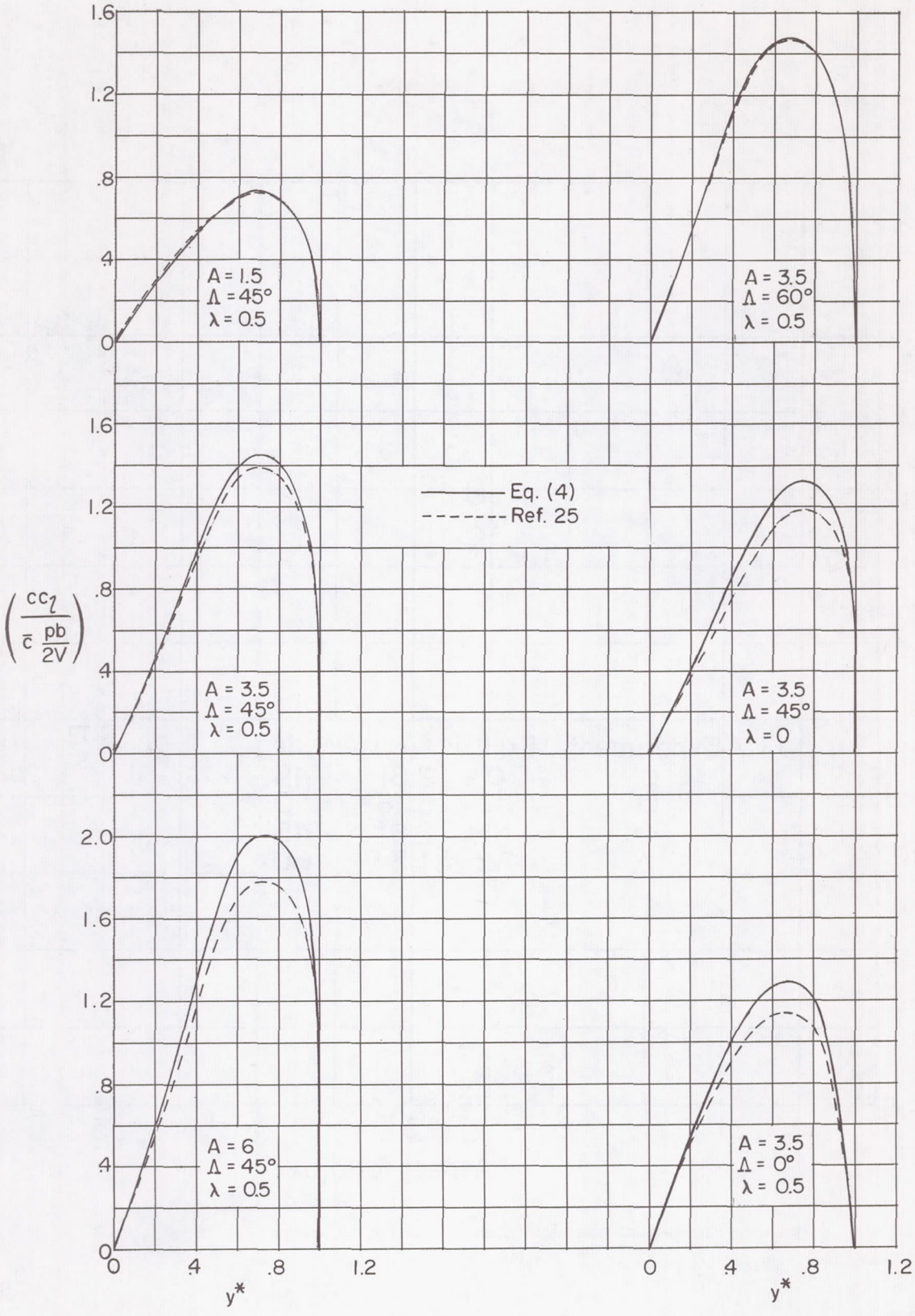

Figure 15.- Computed span-load distribution due to rolling velocity. M = 0.

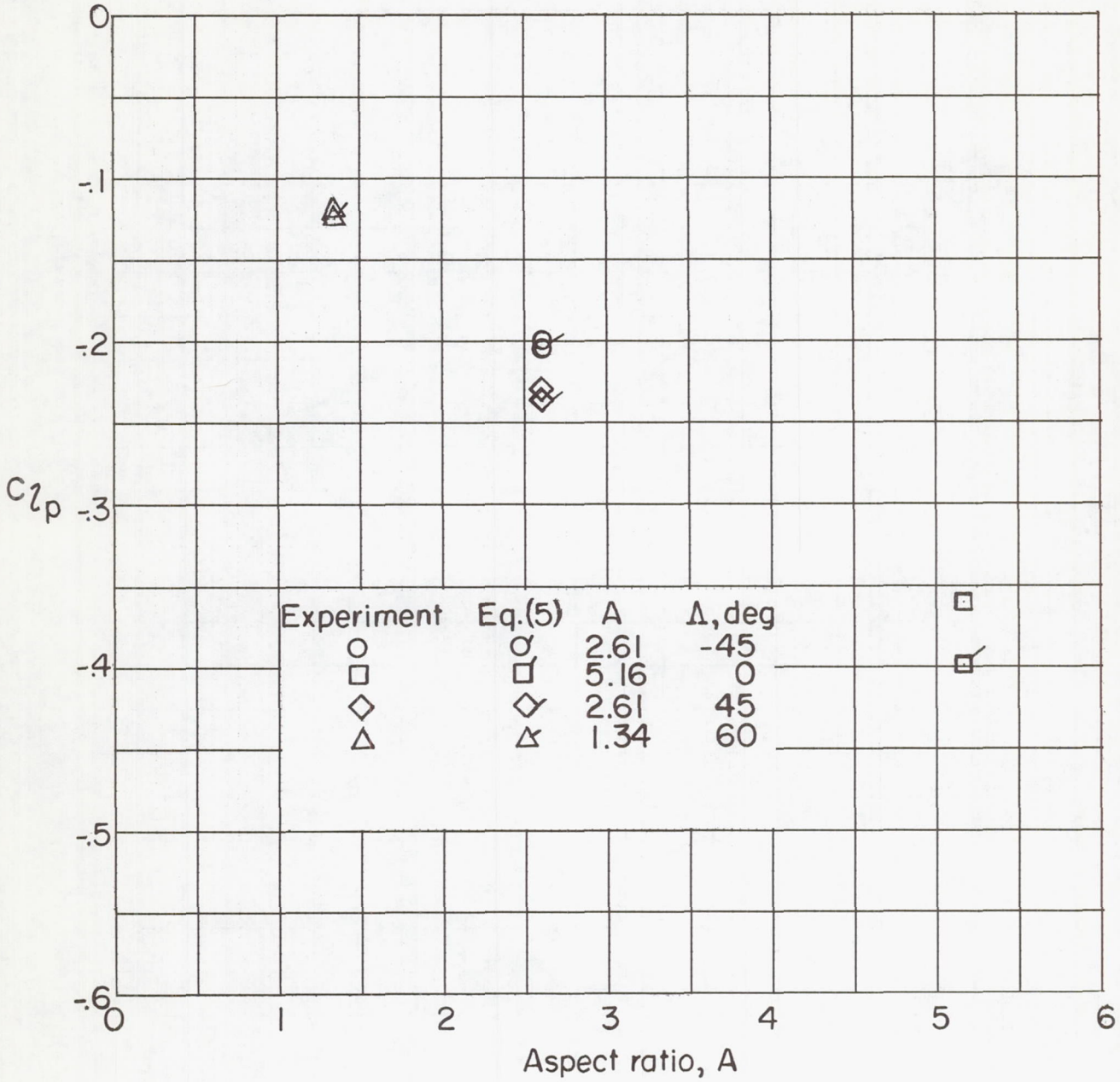

Figure 16.- Calculated and experimental values of damping-in-roll parameter C_{l_p}. M = 0; λ = 1.0.

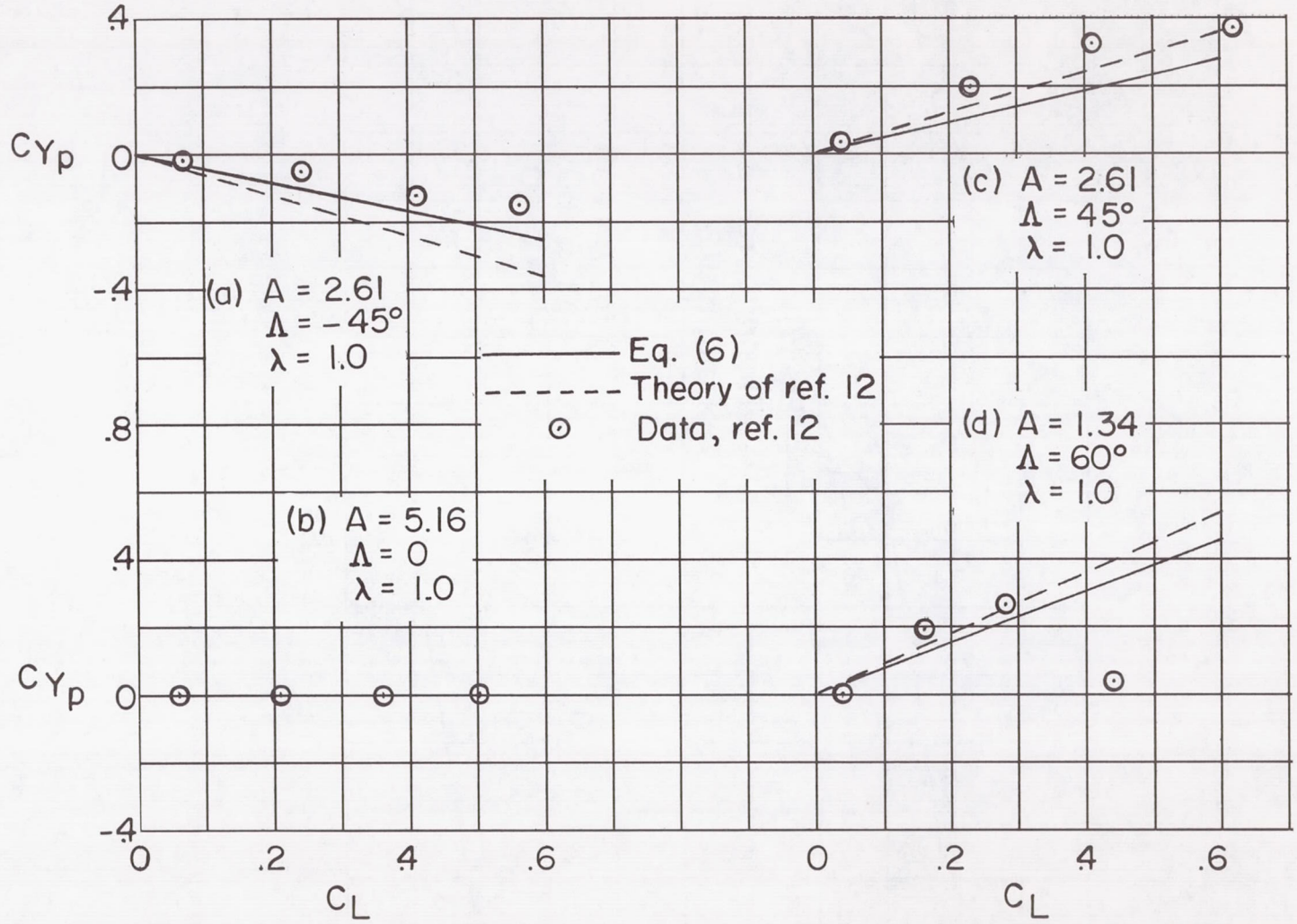

Figure 17.- Theoretical and experimental variations of C_{Y_p} with C_L for several representative wings in incompressible flow.

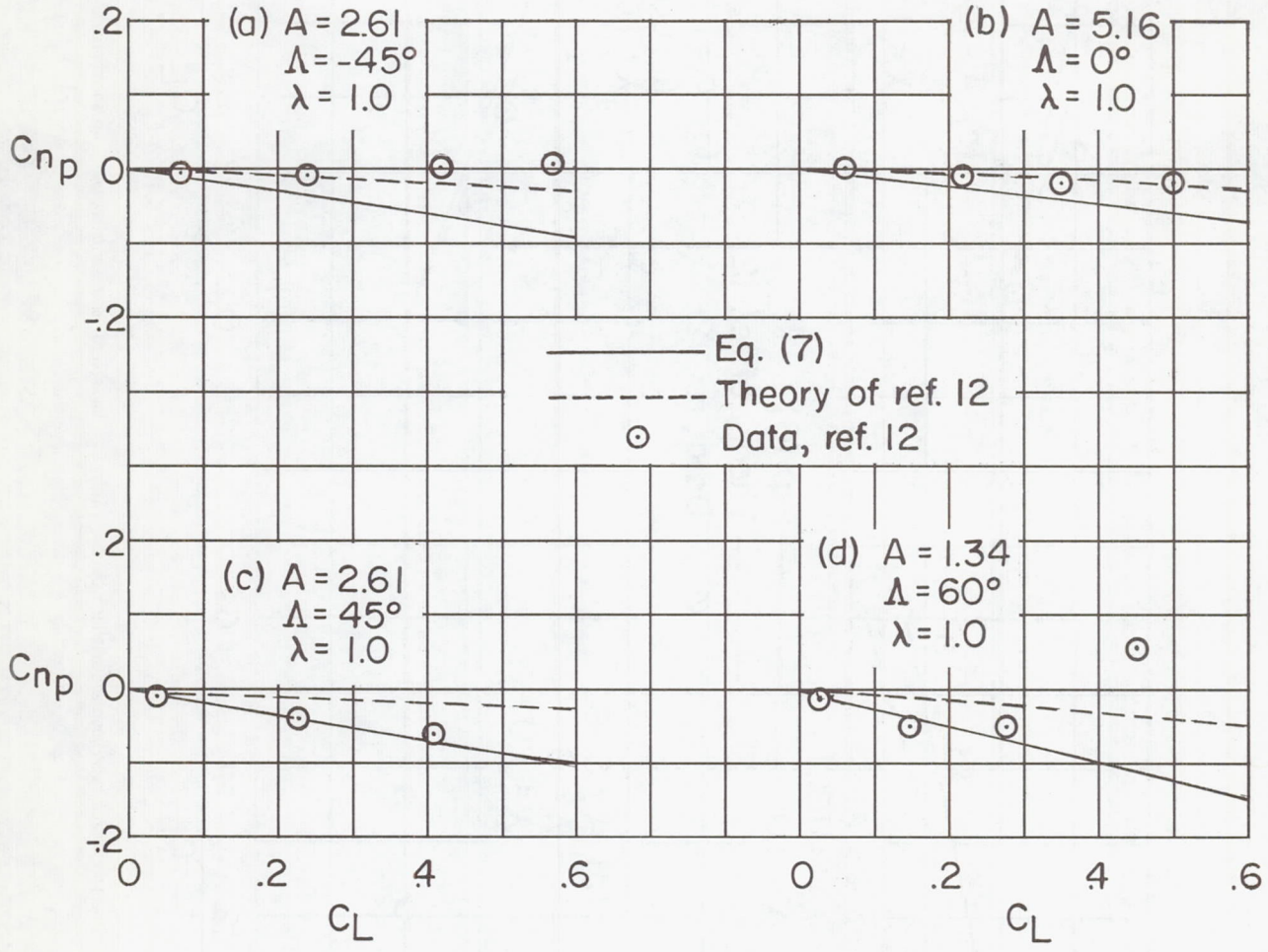

Figure 18.- Theoretical and experimental variations of C_{n_p} with C_L for several representative wings in incompressible flow.

NASA-Langley, 1968 — 1 L-5819